Fall 12-2022

A Biomechanical Analysis of Back Squats: Motion Capture, Electromyography, and Musculoskeletal Modeling

Eva Maria Urdiales Maddox
Old Dominion University, Eva.m.maddox@gmail.com

Recommended Citation

A BIOMECHANICAL ANALYSIS OF BACK SQUATS: MOTION CAPTURE, ELECTROMYGRAPHY, AND MUSCULOSKELETAL MODELING

by

Eva Maria Urdiales Maddox
B.S. May 2013, Austin Peay State University
M.S. May 2015, San Francisco State University

A Dissertation Submitted to the Faculty of
Old Dominion University in Partial Fulfillment of the
Requirements for the Degree of

DOCTOR OF PHILOSOPHY

HUMAN MOVEMENT SCIENCES

OLD DOMINION UNIVERSITY
December 2022

Approved by:

Hunter J. Bennett (Director)

Joshua T. Weinhandl (Member)

Zachary A. Sievert (Member)

ABSTRACT

A BIOMECHANICAL ANALYSIS OF BACK SQUATS: MOTION CAPTURE, ELECTROMYGRAPHY, AND MUSCULOSKELETAL MODELING

Eva Maria Urdiales Maddox
Old Dominion University, 2022
Director: Dr. Hunter J. Bennett

Previous literature evaluating maximal back squats have failed to identify key components of the study decisions and procedures that would allow for duplication. Firstly, the existence of a sticking region in maximally weighted resistance exercises is frequently discussed and has been described as a force-reduced transition phase between an acceleration phase and a strength phase of a lift. However, the etiology has yet to be agreed upon. Second, Electromyography (EMG) is frequently used to assess muscle activations. However, no best practice for EMG normalization has been proposed. Two methods are commonly implemented for normalizing EMG: a maximum voluntary isometric contraction (MVIC) and a dynamic maximum during the task being performed (DMVC). Finally, musculoskeletal modeling software has been increasingly utilized to evaluate muscle forces during weighted back squats. The quality of analyses of muscle forces, excitation, etc. are dependent upon inverse kinematics (IK). However, the methods used when examining IKs have also been short on details making duplication impossible.

This dissertation is in a multiple-article (n=3) format. The first two studies are published in refereed journals. These studies 1) determined the effects of load on lower extremity biomechanics during back squats, 2) examined the influence of normalization method on rectus femoris, vastus medialis, and biceps femoris activations during back squats, and 3) compared different inverse kinematic strategies for calculating hip, knee, ankle, and foot kinematics utilized in modeling of the back squat. For all studies, participants performed the NSCA's one-

repetition maximum (1RM) testing protocol. Three-dimensional motion capture (trunk, pelvis, and lower extremity), force dynamometry (force plates), and EMG were recorded during all squats.

The results of these studies found 1) vertical acceleration was a better discriminative measure than velocity for identifying the sticking region and there is a clear transition from knee to hip dominance for successful maximal squats, 2) the DMVC was more reliable and less variable than MVIC for normalizing EMG, and 3) creating a weld constraint between the foot and the floor results in the most closely matched foot kinematics to the DK results of the methods assessed.

These results indicate that 1) submaximum squats performed at increased velocities can provide similar moments at the ankle and knee, but not hip, as maximal loads, 2) significant emphasis on hip strength is necessary for heavy back squats, 3) normalization to DMVC is the superior method for weighted exercises, and 4) while the Weld model IKs most closely matched the foot DK results, the untenable ankle kinematics the Weld model produced demonstrated it might be the superior choice for modeling foot IKs, but not ankle IKs in maximally weighted back squats.

This dissertation is dedicated firstly to my son Asher, without your distractions and reminders to enjoy life, I would have come out the other side of this a much less fun person. To my husband Chris, you were so supportive, kept me fed, and gave me all the hugs I asked for. To my mom Kerstin, and my dad Guadalupe, growing up you both nurtured my curiosity by never answering my questions simply with "because" and instead encouraged me to find my own answers; you made me the perpetual student that I am. To my best friend Honorine, without you to talk shop and remind me of how cool the human body is, I would have gotten burnt out on all the technical stuff and lost my passion. To one of my favorite people in this world, Blair, who always managed to send me frustrated tirades at the exact moments I needed a laugh. To my stepmom Debbie, and in-laws Jeanne and Max, thank you all for the support and spa gift cards that got me through some of my toughest days. To my always expanding chosen family of friends who were encouraging, supportive and understanding when I had to say no or cancel plans. And finally, to Brandon, who infuriatingly and heartbreakingly reminded me that life is short and should not be taken seriously.

ACKNOWLEDGMENTS

I would like to thank my advisor Dr. Hunter Bennett for his consistent support and encouragement during the past few years. He put up with more than one meltdown and always created a safe space for me to learn and grow. I would not have been successful without your patience and dad jokes.

I would also like to thank my dissertation committee members, Drs. Joshua Weinhandl and Zachary Sievert for their input and guidance, my comprehensive exam committee, Drs. Holly Gaff and Stacie Ringleb for the fun and out of the box questions, and the many professors and fellow students that challenged me along the way.

TABLE OF CONTENTS

LIST OF TABLES

LIST OF FIGURES

CHAPTER 1. INTRODUCTION

Dynamic exercises are widely used in athletics and exercise programs. The back squat is a foundational dynamic exercise because it is biomechanically and neuromuscularly similar to many athletic movements (Gullett et al., 2009; Kubo et al., 2018). Back squats have been extensively researched, evaluating everything from athletic preparedness (Myer et al., 2014; Schoenfeld, 2010) to post surgery recovery (D. S. Catelli et al., 2020). Furthermore, the back squat is a functional, multi-joint, multi-planar exercise that requires coordinated efforts spanning the entire body while utilizing all lower extremity muscle in some capacity (isometric, concentric, or eccentric) (Escamilla, Fleisig, Lowry, et al., 2001; Escamilla, Fleisig, Zheng, et al., 2001; Flanagan et al., 2003; Jaberzadeh et al., 2016; Marshall et al., 2011; Murray et al., 2013; Yavuz et al., 2015). Depending on the goal, various repetition and set schemes of the back squat are implemented. Weight training programs utilize submaximal and supramaximal training and testing to track progress and sport readiness (Duncan et al., 2014; Marshall et al., 2011; Sanborn et al., 2000). Beyond the goal of lifting the largest load possible for specific back squat competitions such as powerlifting, load lifted has been linked to performance in many sport specific settings (Brandon et al., n.d.; Gorsuch et al., 2013; McBride et al., 2009; McCurdy et al., 2010; Miletello et al., 2009; Panariello et al., 1994; Williams et al., 2021). Increasing an athlete's capability to lift larger loads is of interest to all athletic coaches with the goal of improving their athlete's performance. Therefore, understanding what causes an athlete to succeed/fail a back squat needs to be explored.

This multi-article dissertation spans three topics directly pertaining to the evaluation of back squats. First, this dissertation explores "what are the mechanisms that limit success in maximally loaded back squats?" Second, an evaluation of "how muscle activation in maximally

loaded back squats are normalized effects the reported results." Finally, an investigation into "what specific inverse kinematic parameters are required to produce accurately model maximal back squats?"

1. The Sticking Region

The ascent phase of the back squat can be divided into three regions: 1) acceleration, 2) sticking, and 3) strength and deceleration (Escamilla et al., 2000). The sticking region is assumed to be where failure occurs around 30° to 49° thigh angle relative to the ground (Escamilla, Fleisig, Lowry, et al., 2001; Hales et al., 2009). Although there is no consensus on what the sticking region is (Escamilla, Fleisig, Lowry, et al., 2001; Kompf & Arandjelović, 2016; van den Tillaar et al., 2014), some evidence suggests failure at the sticking region might be due to decreased vertical velocity (Escamilla, Fleisig, Lowry, et al., 2001), muscle failure (Elliott et al., 1989; Willardson, 2007), inadequate transition from knee to hip dominance (van den Tillaar, 2015), and/or ill-timed muscle activation (van den Tillaar et al., 2014). In addition to examining what the sticking region is/consists of, many possible mechanisms for failure in the sticking region have been explored (Elliott et al., 1989; van den Tillaar, 2015; Willardson, 2007). Van den Tillaar (van den Tillaar et al., 2014) suggested muscle activation timing between the knee and hip extensors are responsible for failure in the sticking region. In support of this, a previous study that evaluated a failed repetition versus a successful repetition of a three-repetition-maximum squat protocol showed failure was due to hip loading (Flanagan et al., 2015). However, squats were not to full depth and failure was achieved by muscular fatigue (Flanagan et al., 2015). Although previous studies provide some insight into failure of back squats using multi-rep maxes, further research is required to understand increasing loads affects during the back squat. A clear understanding of the ankle, knee, and hip contributions during the

acceleration and sticking regions could enhance training at all levels. The lower extremity moment is comprised of joint loads of 80-90% at the hip and knee and 0-20% at the ankle to lift the system mass during the ascent phase of back squats (Bennett et al., 2020; Escamilla, Fleisig, Lowry, et al., 2001; Flanagan et al., 2015; Flanagan & Salem, 2008; Fry et al., 2003; Hirata & Duarte, 2007; Lorenzetti et al., 2012; Maddox et al., 2020). Furthermore, exploring specific lower extremity muscular involvement in one-repetition-maximum (1RM) squats could elucidate the underlying mechanisms behind failure.

2. Electromyography Normalization

Muscular involvement during movement are commonly analyzed using electromyography (EMG). EMG is frequently used in squat research to determine advantageous movement patterns for muscle activation, methods to decrease knee loading, ways to improve joint alignment, and squat depths (Balshaw & Hunter, 2012; Contreras et al., 2015; Escamilla, Fleisig, Lowry, et al., 2001; Jaberzadeh et al., 2016; Lynn & Noffal, 2012; Murray et al., 2013). Muscular activation during movement is assessed as normalized EMG. Utilization of non-normalized EMG data should be avoided (Besomi et al., 2020). Many factors can affect the EMG signal (i.e. extrinsic and intrinsic causative factors that influence the signal) but can be neutralized with normalization (De Luca, 1997).

Several methods for normalizing EMG are in current use (Besomi et al., 2020). The most frequently used method is obtaining a maximum voluntary isometric contraction (MVIC). However, MVIC normalized EMG is cautioned against if the dynamic maneuver is different than the MVIC procedure (Besomi et al., 2020). EMG can also be normalized to the peak EMG signal of the dynamic task being evaluated (Balshaw & Hunter, 2012). Many dynamic movements present greater peaks in EMG amplitude than in MVIC trials (Ricard et al., 2005; Suydam et al.,

2017). Furthermore, the ascending phase of the back squat presents significantly greater muscle activation than the descending phase (Gullett et al., 2009).

There are important methodological factors to consider when evaluating muscle activation patterns in back squats. Peak EMG of ballistic tasks can produce greater within-participant variability than peak EMG of MVIC tasks for each muscle (Suydam et al., 2017). Of the studies evaluating EMG normalization, most have provided support for (Allison et al., 1993; A. Burden & Bartlett, 1999; A. M. Burden et al., 2003; Chapman et al., 2010; Kashiwagi et al., 1995; Knutson et al., 1994; Yang & Winter, 1984) with very few being against (Bolgla & Uhl, 2007) the usage of a dynamic maximum for EMG normalization. Additionally, it has been shown that maximal loading is required for full activation of muscles (Yavuz et al., 2015), which suggests a dynamic maximum voluntary contraction (DMVC) is a more applicable normalization technique than MVIC for maximally weighted back squats (Besomi et al., 2020). Furthermore, normalizing to a submaximum back squat trial demonstrated greater absolute reliability for both the vastus lateralis (7.6 ± 1.1 – 10.2 ± 0.6 CV%) and the biceps femoris (12.6 ± 3.5 – 18.9 ± 4.1 CV%) compared to MVIC (24.3 ± 0.5 and 28.5 ± 1.1 CV%, respectfully) (Balshaw & Hunter, 2012). Non-squat studies found normalizing to a dynamic trial is a more reliable normalization technique (Albertus-Kajee et al., 2011; Clarys, 2000; Suydam et al., 2017).

There are several factors that need to be considered if using dynamic maximums instead of MVICs for normalization of dynamic EMG data: 1) small alterations in technique could affect activations compared to previous assessments, 2) not all maneuvers will produce maximal muscle activation, and 3) repeating dynamic maximums could cause undue fatigue. Consideration of normalization procedure is also crucial for between-participants' comparisons, as it could affect group-based comparisons. Currently, no normalization method is universally

adopted, likely due to previous mixed results. As such, a detailed comparison of each normalization scheme is warranted. Furthermore, muscular activation assessments of failed attempts of maximally weighted back squats during the sticking region are likely susceptible to normalization scheme.

3. Modeling Overview

Despite the important information that can be gleaned from EMG analyses, they are limited in that muscle activation does not equate to muscle forces for dynamic movements. Muscle forces cannot be measured in vivo without the use of invasive techniques such as buckle transducers that are inserted into the muscular-tendon unit (Karabulut et al., 2020). Instead, equations-of-motion driven musculoskeletal models are implemented to predict in-vivo loads. While many options are available, the most frequent musculoskeletal modeling software platform is called OpenSim and can be used to estimate the muscle forces required to produce the dynamic movements of the body (Hicks et al., 2015). Musculoskeletal models that have been developed for OpenSim have been used to calculate and/or estimate numerous biomechanical aspects of many different movements (Abelbeck, 2002; Deaux & Engstrom, 1973; Delp et al., 2007; Reinbolt et al., 2011; Seth et al., 2011, 2004; Singh & Padgham, 2014). In particular, extensive research has been conducted using models in the OpenSim environment evaluating walking gait (Anderson & Pandy, 2003; Lai et al., 2017; Lin et al., 2010; Rajagopal et al., 2016), running gait (Dorn et al., 2012; Fiorentino et al., 2014; Hamner et al., 2010), throwing (Golfeshan, Barnamehei, Rezaei, et al., 2020; McConnell et al., 2011), jumping (Earp et al., 2010), landing (Boozari et al., 2020), cycling (Park et al., 2022), injury (D. S. Catelli, 2018; Schache et al., 2009), surgery (Delp & Zajac, 1992; Herrmann & Delp, 1999), and many others (Arandjelović, 2010; Butler et al., 2017; Jung et al., 2017; Shelburne & Pandy, 2002). A brief on

the steps to perform a modeling analysis within OpenSim using experimentally collected marker trajectories (i.e., segmental kinematics) and GRFs is provided below.

To improve subject specificity, musculoskeletal models are scaled to match a research study participant's anthropometrics. In some cases, the exact locations of joint centers, and/or bone geometries can be defined using magnetic resonance imaging to create a model as closely matching the bone geometries of a participant as possible (Modenese & Renault, 2021). This is particularly important if the musculoskeletal model is being used to predict the resultant muscle behavior after a surgical intervention (Delp & Zajac, 1992; Herrmann & Delp, 1999). Typically, however, the musculoskeletal model is scaled using segment lengths determined via three-dimensional motion capture where joint center locations estimated using bony landmarks and/or predictions from regressions and functional movement analyses (Bennett et al., 2016). Muscle parameters can also be specified to a participant using techniques like ultrasound and magnetic resonance imaging (Arnold et al., 2000; Barnamehei et al., 2022; Fernandes de Oliveira & Luporini Menegaldo, 2010; Gerus et al., 2015; Smale et al., 2019). The database informed muscle characteristics can predict the possible muscle forces required for the model to conduct a specific movement (Akhundov et al., 2022; Kramer et al., 2022).

The model's kinematics are matched as closely as possible to an experimentally three-dimensional motion captured movement of a participant. The model's kinematics are created using a method called inverse kinematics. Inverse kinematics uses the three-dimensional motion capture data, a subject specific model, and marker weights to maximize the matching of the model's kinematics to the experimentally collected data. Marker weights are used to "prioritize" which markers to match as closely as possible between the data and the model. The higher the weight, the less error the model will attempt to achieve. The model's inverse kinematics are

combined with experimentally collected ground reaction forces to calculate the net forces produced at each joint. Subsequently, the analysis tool can be used to calculate the possible forces each muscle would contribute to the movement. Thus, the muscle force predictions required to move the scaled model through the matched movement can be inferred to be the muscle forces within the living participant (Lamas et al., 2022; Mokhtarzadeh et al., 2014).

4. Modeling Squats

Modeling has been used to predict internal forces occurring during squatting maneuvers for decades (Dahlkvist et al., 1982). However, full depth back squats require larger joint angle ranges in the hip (>140°), knee (>130°), and ankle (>40°) than the ranges of the movements that have been modeled in the past (Hemmerich et al., 2006; Maddox & Bennett, 2021). Because of the inadequate ranges of motion available in the current musculoskeletal models, alterations needed to be made. Recently, musculoskeletal models designed for squatting maneuvers have been developed: Lai2017 (Lai et al., 2017) then Catelli2019 (D. S. Catelli et al., 2019). Prior to Lai et al., there were several issues with musculoskeletal models: 1) overestimation of passive fiber forces by the hip and knee extensors, 2) poor representations of muscular properties over their entire range-of-motion, and 3) muscles becoming unrealistically short during high flexion and not producing force. Lai et al. used the Rajagopal2015 model as the base to adjust and allow larger knee ranges-of-motion. The alterations made to the Rajagopal2015 model were: 1) an update to the tibiofemoral kinematics, 2) increased knee flexion capabilities from 120° to 140°, 3) updated the origin-to-insertion paths of knee muscles, 4) increased knee translation when flexed more than 60°, 5) updated attachment points and wrapping surfaces of muscles about the knee joint, and 6) modified the paths of the biceps femoris short head and the lateral gastrocnemius. The alterations allow for the large knee motions required to improve muscular

predictions for deep ranges-of-motion maneuvers like the squat. However, when evaluating dynamic movements, muscle excursions of the gastrocnemii were far greater than excursions measured with ultrasound and unlikely passive forces and co-activation of muscles were produced that were inconsistent when compared to EMG (Lai et al., 2017).

The Catelli2018 model further updated the Lai2017 model by adjusting wrapping surfaces for muscles at the knee and hip joints to allow for the required large hip and knee flexion to complete a deep squat maneuver (D. S. Catelli et al., 2019). The alterations made to the Lai2017 model were: 1) increased hip flexion capabilities from 120° to 138°, 2) increased knee flexion capabilities from 140° to 145°, 3) updated the wrapping surfaces of six muscle-tendon units, 4) added two wrapping surfaces to each of nine muscle-tendon units to prevent bone crossing, and 5) added an additional wrapping surface to the rectus femoris and sartorius to prevent bone crossing at the head of the femur. When compared to the original Lai2017 model, no differences in kinematics were found. Furthermore, the addition of the wrapping surfaces allowed the model to achieve large hip flexion (120.2°), abduction (13.7°), and external rotation (19.6°), and knee flexion (142.2°) angles without the muscles crossing the bones. When used to evaluate squat depth in Asian compared to Caucasian subjects, the Catelli2018 model produced comparable muscle activation estimations to experimentally measured EMG (Y. Lu et al., 2020).

Several recent studies (Bedo et al., 2020; Bini et al., 2021; D. S. Catelli et al., 2020; Golfeshan, Barnamehei, Torabigoudarzi, et al., 2020; Kipp et al., 2022b; Li et al., 2021; Song et al., 2022; Wolf et al., 2021) have evaluated squat maneuvers using the updated musculoskeletal models outlined above (Lai2017 and Catelli2019). These previous studies focused on the hip and knee with little to no attention paid to the ankle. The focus on hip and knee joints is likely because a majority of the load (i.e., moments) during a back squat is carried at the hip (~50%)

and knee (~30%) (Maddox & Bennett, 2021). Loading at the ankle is small in comparison (~20%); however, the ankles are important for proper movement mechanics (Demers et al., 2018; Fuglsang et al., 2017; Gomes et al., 2020; Maddox & Bennett, 2021). Ankle dorsiflexion range-of-motion is significantly associated with back squat depth (Gomes et al., 2020), with greater dorsiflexion functionality allowing for deeper squats. Additionally, ankle muscle stiffness regulation is required for maintenance of ankle stability during dynamic movements (Pangan & Leineweber, 2021; Xie et al., 2021). Xie et al., reported increased ankle stiffness during the stance phase of walking with an increase in surface compliance, indicating a relationship between ankle stiffness and the need to maintain lower extremity stability during dynamic movements. Pangan, et al., concluded that greater ankle dorsiflexion during a squat on an unstable surface is an attempt to maintain stability at the ankle. These characteristics emphasize the importance of including the ankle when evaluating back squat mechanics.

Ankle biomechanics during squats have been evaluated using OpenSim models (Bini et al., 2021; Bordron et al., 2021; Golfeshan, Barnamehei, Torabigoudarzi, et al., 2020; Li et al., 2021; Wolf et al., 2021). Bini et al., 2021 reported no significant differences in mean sagittal plane moments of the ankle when performing squats to parallel. However, the study reported high inter-participant variability for all joint moments (Bini et al., 2021). Li et al., 2021 evaluated range-of-motion and peak moments for hips, knees, and ankles, and found significantly larger range-of-motions for all three joints during the full depth squat than the half squat (Li et al., 2021). Furthermore, larger peak knee extension and hip extension moments were observed during the full squat than the half squat, whereas peak ankle plantarflexion moments were larger during a half squat than a full depth squat. Wolf et al., 2021 investigated relative muscular effort (the ratio between net joint moments and maximum net joint moments) and net moments for the

hip, knee, and ankle joints. No significant difference in ankle relative muscular effort between external loads was found (Wolf et al., 2021). In another study that evaluated muscle forces, Golfeshan et al., 2020 reported significant differences in medial gastrocnemius forces between hands-behind-the-head and hands-in-front-of-the-chest bodyweight squats. The information presented in these studies provides some understanding of what may be occurring at the ankle during squats; however, these studies provided surprisingly little to no information regarding the details of their inverse kinematic modeling procedures, making evaluation and replication very difficult.

Inverse dynamics, muscular analyses, and joint reaction forces calculations using musculoskeletal models rely heavily on the accuracy of model-specific kinematic solutions (Riemer & Hsiao-Wecksler, 2008). With the foot being the point of contact in a squat, any inaccuracies could have critical impacts on all subsequent analyses. Any unexpected displacement of the foot during data collection could likely be attributed to model defined constraints (assuming no user error). When using musculoskeletal modeling for full depth squats, improper kinematic solutions can unrealistically plantarflex the feet through the floor during the descent phase of the back squat (Figure 1). Given we found this issue with each of the aforementioned models, it is likely previous studies also had issues with the feet and did not mention it in their publication or compensated for the issues by modifying procedures such as weight schemes for inverse kinematics. In fact, a recent study implemented a weld joint between the foot and the floor using the Rajagopal Model (Rajagopal et al., 2016), indicating they too may have experienced issues with plantarflexion of the model (Bordron et al., 2021). However, no indication of why they used a weld joint was included in the final publication.

Figure 1. Visualization of model issue.
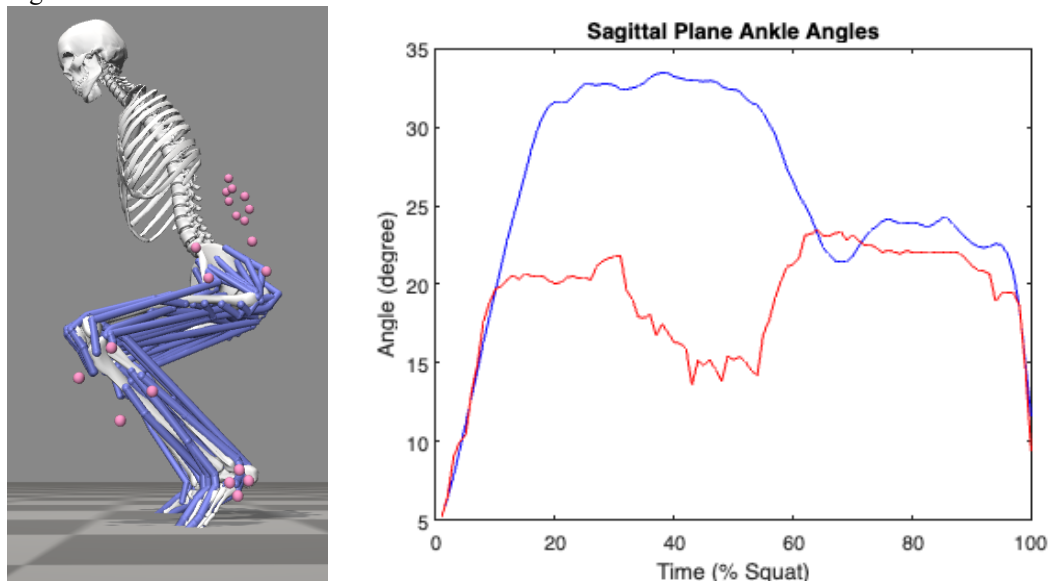
Left: Example of Catelli model performing back squat. Right: Sagittal plane ankle angles of a representative subject (direct kinematics in blue, inverse kinematics using OpenSim in red).

Thus, a study evaluating different inverse kinematic procedures of a weighted back squat is warranted. Three specific procedures are likely the most applicable. First, a weighted inverse kinematics solution. Second, altering the model to include a weld joint between the feet and the floor. Third, utilizing a toe marker during dynamic trials. Finally, an unweighted least-squares inverse kinematics evaluation will serve as a control procedure. Which is important because many of the current studies do not report any weighting of the least-squares inverse kinematic evaluation that may have been included.

Of the three procedures, the foot-floor weld procedure will likely produce the most closely matched results compared to experimentally collected data. A recent study used segment lengths to normalize the weighting scheme for their inverse kinematics analysis and created a weld joint between the foot and the floor, indicating they too may have experienced issues with plantarflexion of the model (Bordron et al., 2021). While the study estimated joint moments compared to calculated joint moments, no kinematic data was reported.

5. Purpose of the Studies

This dissertation is in a multiple-article format. The first two studies are published in refereed journals. The purpose of the first study was to evaluate the effects of weighted back squat load on velocity and acceleration of the center-of-mass, as well as joint angles and moments during the acceleration and sticking regions of the ascent phase. The purpose of the second study was to determine the intra- and inter- group muscle activity variability and reliability effects of two electromyography normalization methods. The purpose of the third study is to evaluate the effects of inverse kinematic evaluations on the resultant ankle and foot kinematics using the OpenSim software.

6. Research Questions

1. How does increased external load affect the biomechanics of the lower extremity during the ascent phase of the back squat?

2. Which electromyography normalization method results in the lowest intra- and inter- group variability and greatest intra- and inter- group reliability?

3. Can an informed inverse kinematic method improve ankle and foot kinematic analyses of back squats?

7. Significance of the Studies

The first study elucidated metrics and possible training focal points for athlete successful completion of maximally weighted back squats. The second study identified a superior electromyography normalization method for weighted back squats. The third study established the best inverse kinematics method for evaluating lower extremity kinematics using a musculoskeletal software.

8. Delimitations

1. Criteria for inclusion in the study was purposefully limited to healthy participants between 18 and 55 years of age with no history of knee injuries, at least one-year experience performing back squats at near maximal loads for at least one-day per week.

2. All participants were instructed to use a shoulder-width stance when performing each repetition.

3. Full depth was defined as contact between posterior thigh and shank at the bottom of the squat, with a researcher instructing the participant when to ascend from the bottom of the squat to ensure bouncing at the bottom of the squat did not happen.

4. All participants wore lab issued shoes (Nike).

5. Participants were instructed to not perform lower body weight training for 48-hours prior to testing sessions.

9. Limitations

1. Participants were not elite level weightlifters, which could result in disparities in technique.

2. The warmup was not standardized. Each participant was able to perform a warmup of their choosing.

CHAPTER 2. EFFECTS OF EXTERNAL LOAD ON SAGITTAL AND FRONTAL PLANE LOWER EXTREMITY BIOMECHANICS DURING BACK SQUATS

Abstract

Previous literature suggests the sticking region in barbell movements may be the reason for failing repeated submaximal and maximal squats. Although the existence of a sticking region is frequently discussed, the etiology has yet to be agreed upon. The sticking region has been loosely defined as a force-reduced transition phase between an acceleration phase and a strength phase of a lift This study determined the effects of load on lower extremity biomechanics during back squats. Twenty participants performed the NSCA's one-repetition maximum (1RM) testing protocol, testing to supramaximum loads (failure). A 1RM is the maximal amount of weight that can be lifted in a single repetition. After completing the protocol and a 10-minute rest, 80% 1RM squats were performed. Statistical parametric mapping was used to determine vertical velocity, acceleration, ankle, knee, and hip sagittal and frontal plane biomechanics differences between 1RM, submaximum, and supramaximum squats (105% 1RM). Vertical acceleration was a better discriminative measure than velocity, exhibiting differences across all conditions. Supramaximum squats emphasized knee moments, whereas 1RM emphasized hip moments during acceleration. Submaximum squats had reduced hip and knee moments compared to supramaximum squats, but similar knee moments to 1RM squats. Across all conditions, knee loads mirrored accelerations and a prominent knee (acceleration) to hip (sticking) transition existed. These results indicate that 1) submaximum squats performed at increased velocities can provide similar moments at the ankle and knee, but not hip, as maximal loads and 2) significant emphasis on hip strength is necessary for heavy back squats.

1. Introduction

The back squat is a widely used exercise in both athletics and other exercise programmes. The back squat is a functional, compound and multi-joint exercise that targets all major muscle groups of the lower body (Flanagan et al., 2003). Because of the benefits provided by back squats to general sport readiness (Schoenfeld, 2010), strength & conditioning coaches everywhere likely implement some form of squats in their exercise programmes. The back squat is similar in biomechanical and neuromuscular parameters to a multitude of athletic movements (Gullett et al., 2009; Kubo et al., 2018).

Given the benefits and translation across acitivities, weight lifting programs implement one-repetition-maximum (1RM) and submaximum (to failure) back squat tests to track progress of athletes' strength, muscle hypertrophy, and sport readiness (Seitz et al., 2014). The back squat requires participation of every lower extremity muscle in some capacity (isometric, concentric, or eccentric) (Escamilla, Fleisig, Lowry, et al., 2001; Escamilla, Fleisig, Zheng, et al., 2001; Jaberzadeh et al., 2016; Marshall et al., 2011; Murray et al., 2013; Yavuz et al., 2015). In general, the loads for the hip and knee joints comprise 80-90%, whereas the ankle contributes 0-20%, of the total lower extremity moment to lift the system mass during the upward portion of back squats (Escamilla, Fleisig, Lowry, et al., 2001; Flanagan et al., 2015; Flanagan & Salem, 2008; Fry et al., 2003; Hirata & Duarte, 2007; Lorenzetti et al., 2012). Various repetition and set schemes for the back squat may be implemented depending on the training goal, including submaximal and supramaximal training (Duncan et al., 2014; Marshall et al., 2011; Sanborn et al., 2000).

The upward phase of the back squat can be split into three regions: 1) acceleration, when vertical bar velocity is increasing from at-depth to peak positive velocity, 2) sticking, vertical

velocity decreases to a local minima, and 3) strength and deceleration, culminating in the greatest

peak velocity followed by completion to standing upright (Escamilla et al., 2000; Figure 2).

While the sticking region is frequently assumed to be the area where success/failure occurs, there

is no consensus on what the sticking region is other than the most difficult region of the barbell

lift (Escamilla, Fleisig, Lowry, et al., 2001; Kompf & Arandjelović, 2016; van den Tillaar et al.,

2014). There are many possibile mechanisms driving the sticking region (e.g. proper transition

from knee to hip dominance (van den Tillaar, 2015) or muscular failure (Elliott et al., 1989;

Willardson, 2007); however, there is no consensus as how the sticking region is overcome.

Figure 2. Barbell velocity during concentric phase of the back squat
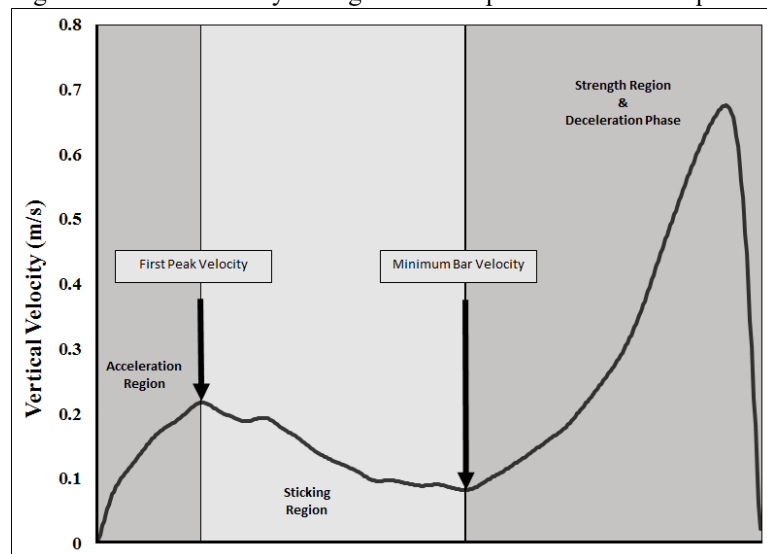
The plot above depicts vertical velocity of the barbell during the concentric phase of the back squat: from full depth to standing upright. There are three distinct regions of the concentric phase: Acceleration, Sticking, and Strength/Deceleration. The Acceleration Region contains the velocity profile from full depth to the first peak. The Sticking Region begins at first peak and ends at minimum bar velocity. The Strength/Deceleration Regions contain the 2nd peak velocity.

In the squat, the sticking region appears to occur around 30° to 49° thigh angle relative to

the ground (Escamilla, Fleisig, Lowry, et al., 2001; Hales et al., 2009). Van den Tillaar (van den

Tillaar et al., 2014) suggested that the timing of muscle activation between the knee extensors

and the hip extensors are responsible for the sticking region in the squat using a 6-RM squat

protocol. Their work found biceps femoris activity increased during the activation region to

sticking region, with a transition to the rectus femoris increasing from the sticking region through the strength phase (van den Tillaar et al., 2014). However, they did not analyze any different loads. Only one previous study has included failed versus successful 1RM squats (Flanagan et al., 2015). In Flanagan, et al. the, failure, on the group level, was due to hip loading (Flanagan et al., 2015). However, there are several important aspects to note regarding the Flanagan, et al. study: 1) there were only five participants included in the pass/fail examination, 2) squats were performed to parallel, and 3) failure was achieved by muscular fatigue, not through increasing external loads (Flanagan et al., 2015). Although the previous works provide some insight into back squats using multi-rep maxes at various levels, further research is required to understand how the lower extremity system responds to increasing loads during the back squat, particularly within the acceleration and sticking regions. From a coaching perspective, defining the relationship between performance (e.g. vertical velocity) during concentric phase and lower extremity biomechanics could be useful in deriving focused training protocols to improve strength in back squats. In addition, a clear depiction of the ankle, knee, and hip contributions to the lower extremity support moment (total moment) during the acceleration and sticking regions could enhance localized training at both sub-maximum and maximum levels.

  Therefore, the purpose of this study was to determine how loading affects performance (whole-body velocity and acceleration) and joint level biomechanics (angles and moments) during the acceleration and sticking regions of back squats. We hypothesised that 1) a clear knee to hip transition during the sticking region, evidenced by greater contributions to the total lower extremity moment, would occur for submaximum and 1RM squats but be muted in

supramaximum squats and 2) reduced vertical velocity would be evident in both the acceleration and sticking regions in supramaximum compared to both 1RM and submaximum squats.

2. Methods

2.1. Participants

The study was approved by the Old Dominion University Institutional Review Board. Twenty resistance-trained individuals were recruited from the local fitness community, including the university campus using flyers/advertisements and word of mouth. Inclusion criteria included: healthy with no history of knee injuries, age 18-55 years, must perform weighted squats at least 1 day per week, and at least one-year experience back squatting at or near maximal loads. Exclusion criteria included: any lower extremity injuries in the past 3 months, knee pain in the past 6 months, a diagnosis of lower extremity joint arthritis, or a body mass index (BMI) greater than 35 kg·m-2. All participants were informed of the study procedures and signed consent forms. All participants were screened with a standard Physical Activity Readiness Questionnaire (PAR-Q); this questionnaire covers any unrelated health issues that may be of concern. All participants donned a pair of spandex shorts and standardized laboratory shoes (NIKE Airmax Glide). Participant demographics are provided in Table 1.

Table 1. Participant demographics: mean ± standard deviation

	Body Mass (kg)	Submax (BMs)	1RM (BMs)	Supramax (BMs)
Overall (n=20)	80.53±14.28	1.08±0.19	1.35±0.24	1.42±0.25
Males (n=10)	85.87±11.06	1.18±0.13	1.47±0.16	1.55±0.16
Females (n=10)	75.19±15.65	0.98±0.20	1.23±0.25	1.28±0.24

Resistances were normalized to body mass (BMs). Submax resistances were set at 80% 1RM. Supramax resistances averaged 105% 1RM resistance (range: 103-107% 1RM).

2.2. Procedures

A ten-camera motion capture system (200Hz, Vicon Motion Analysis Inc., Oxford, UK) was used to collect three-dimensional (3D) kinematics. Retroreflective anatomical markers were

placed bilaterally on the iliac crests, anterior superior iliac spines (ASISs), posterior superior iliac spines (PSISs), greater trochanters, femoral epicondyles, medial and lateral tibia condyles, medial and lateral malleoli, 1st and 5th metatarsal heads, and 2nd toes. Clusters of four tracking markers were attached to the pelvis, thighs, shanks and shoe heels. The anatomical and tracking markers were used to create a biomechanical model consisting of 7-segments (pelvis, thighs, shanks and feet) with six degrees of freedom each. A traditional style barbell rack, barbell (20.5 kg) and weighted plates were placed around the center of the motion capture collection area and two force platforms (2000Hz, Bertec FP-4060, Bertec Inc. OH, USA). Force platforms collected ground reaction forces (GRFs) applied to the foot segments (both feet) during the entirety of each squat repetition.

Prior to beginning the 1RM testing, participants were allowed five minutes for warming up and stretching of their choice. Next, participants completed the NSCA's 1RM testing protocol (Haff & Triplett, 2016). Participants were given 20 minutes to warm up to their 1RM. After several warmup sets of progressively greater resistance a 1RM was attempted. If successful, the subject rested 2-4 minutes and 30-40 lb or 10-20% increase was made for another attempt. If the subject failed, 2-4 minutes of rest was given and the weight was reduced by 15-20 lb (7-9kg) or 5-10% and a 1RM was attempted again, until an official laboratory 1RM was found (Table 1 contains 1RM data normalized to body mass). The failed attempt closest to their laboratory 1RM was used as the Supramaximum trial in this study (range: 103-107% 1RM; Table 1). After completion of the 1RM protocol and a subsequent rest period of at least 10 minutes, participants performed a back squat with 80% of their 1RM (Submaximum; Table 1).

Participants were instructed to squat with shoulder-width stance and descend to full depth (contact between posterior thigh and shank). "Bouncing" out of the bottom of the squat was not

permitted and was regulated by a command of, "one, up," when full depth was achieved. Participants were not permitted to wear any other gear (weightlifting shoes, belts, etc.). Spotters were used on each side of the participant during all lifts. Participants were directed to avoid any lower body resistance training for 48-hours before the session.

2.3. Data Analysis

All kinematic and GRF data were imported into and processed in commercial biomechanics software, Visual 3D Biomechanical Suite (v6.0, C-Motion, Germantown, MD). Three-dimensional marker trajectories and GRFs were filtered at a cut-off frequency of 5 Hz using a zero-lag fourth-order Butterworth low-pass filter (optimal cutoff calculations of kinematic data using residual analyses agreed with previous work (Escamilla, Fleisig, Lowry, et al., 2001)). A seven-segment model (each with 6 degrees of freedom) was constructed from each subject's static trial data (Bennett et al., 2018). The Davis method was used to determine hip joint centers (Bennett et al., 2018; Davis III et al., 1991). Knee and ankle joint centers were defined as the midpoint of the femoral epicondyles and malleoli, respectively. Joint angles were computed using direct kinematics. An X-Y-Z (flexion-adduction-internal rotation) Cardan rotational sequence was used for 3D angular kinematics computations. The conventions of 3D kinematic and kinetic variables were determined with the right-hand rule. Internal joint moments were calculated using bottom-up inverse dynamics, normalized to body mass (Nm/kg), and expressed in the distal segment. Variables of interest included vertical center of gravity (COG; derived from ground reaction forces) velocity, vertical COG accelerations (derived from ground reaction forces), sagittal and frontal plane angles and moments for the ankle, knee, and hip joints during the concentric phase of the lift. In addition, we analyzed the lower extremity support moment and individual joint contributions to the support moment. The support moment was

derived as the sum of hip, knee, and ankle sagittal and frontal plane moments (absolute values). Waveforms of all variables were normalized from full depth until vertical velocity reached zero (failed squats). Zero vertical velocity was chosen as the endpoint as it is somewhat of a "point of no return" during the lift, occurring immediately prior to the beginning of failure (negative velocity/person going downwards). For successful squats, the global minimum was chosen. To allow for congruency with previous literature, peak (maximum and minimum) sagittal and frontal plane biomechanics are also presented in Tables 2 and 3.

Table 2. Peak sagittal plane ankle, knee, and hip biomechanics from full depth to minimum velocity: mean±std

Joint	Variable	Angles (deg)			Moments (Nm/kg)		
		1RM	Supramax	Submax	1RM	Supramax	Submax
Ankle	Max	24.0±4.2	24.4±4.5	25.2±4.1	-0.60±0.34	-0.81±0.30	-0.66±0.19
	Min	12.9±5.2	17.5±5.8	16.1±6.3	-1.28±0.27	-1.32±0.27	-1.17±0.28
Knee	Max	-73.4±13.1	-93.5±16.8	-75.3±14.3	2.40±0.71	2.49±0.78	2.28±0.86
	Min	-117.1±12.8	-118.4±13.8	-120.0±12.2	1.14±0.40	1.38±0.40	1.18±0.35
Hip	Max	94.1±22.0	94.0±21.8	95.6±22.1	-2.25±0.41	-2.29±0.52	-1.94±0.36
	Min	69.5±19.8	85.1±20.2	73.2±19.3	-2.97±0.48	-3.03±0.49	-2.64±0.46

Angles and moments follow the right-hand rule. Moments are internal and normalized to body mass (kg). Max and min represent the global maximum and minimum values for each variable.

Table 3. Peak frontal plane ankle, knee, and hip biomechanics from full depth to minimum velocity: mean±std

Joint	Variable	Angles (deg)			Moments (Nm/kg)		
		1RM	Supramax	Submax	1RM	Supramax	Submax
Ankle	Max	-0.3±7.0	-4.3±7.8	-2.0±6.7	0.04±0.13	0.04±0.14	0.04±0.13
	Min	-11.3±8.0	-12.7±7.9	-12.8±7.6	-0.21±0.13	-0.11±0.13	-0.12±0.10
Knee	Max	13.8±6.0	13.7±5.9	14.4±6.4	0.25±0.33	0.17±0.30	0.17±0.31
	Min	4.8±5.4	7.8±4.8	7.9±6.0	-0.37±0.18	-0.19±0.35	-0.38±0.19
Hip	Max	-14.9±7.5	-19.1±8.8	-17.5±7.4	0.59±0.40	0.58±0.39	0.58±0.38
	Min	-28.4±8.2	-28.6±8.3	-29.7±7.2	-0.28±0.33	0.13±0.36	-0.15±0.26

Angles and moments follow the right-hand rule. Moments are internal and normalized to body mass (kg).

2.4. Statistical Analyses

All data were imported into Matlab (R2016B, The Mathworks Inc., Natick, MA). Statistical parametric mapping (SPM) was implemented using the open-source spm1d code (v.M0.1, www.spm1d.org). SPM was chosen as the primary statistical assessment over discrete variable analyses because SPM allows assessment of full waveforms, thus simultaneously comparing the timing and magnitude of each variable across loads/conditions. In this respect, the effects of external loading on knee kinematics could be found as increased/reduced motion and/or delays in the occurrence of motion. Prior to implementing comparison tests, normality was assessed using the open-source software and Shapiro-Wilk's statistic. Next, SPM within-participants analysis of variances (ANOVAs) were performed. The statistical parametric map was created using the scalar output statistic, SPM{f}, for each time point. To test the null hypothesis, a critical threshold SPM{f} was computed such that only 0.4% of smooth random curves would exceed the threshold (i.e. alpha at <0.004, reduced from 0.05 to control for multiple tests). When normality concerns were present, non-parametric tests were performed. Supra-threshold clusters were identified as multiple adjacent points of the SPM{f} curve exceeding the 0.4% threshold. In a similar manner, post hoc paired samples t-tests (alpha level at 0.004) were performed when supra-threshold clusters were found.

3. Results

Ensemble waveforms, statistical parametric maps, supra-threshold clusters, and corresponding p-values are presented in Figures 3-8. The ANOVA and post hoc test results for kinematic and kinetic waveforms are provided in Tables 4 and 5. Post-hoc results, including achieved p-values and the mean difference between conditions during the reported statistically significant time range, are discussed below.

3.1. Body-Level Kinematics

Submaximum had increased vertical velocity compared to 1RM from 36-100% (p<0.001, 0.12 m*s-2H-1) and Supramaximum from 26-100% (p<0.001, 0.12 m*s-2H-1) depth to minimum velocity (Figure 3a; Table 4). Supramaximum had decreased vertical acceleration compared to 1RM from 65-100% (p<0.001, 0.34 m*s-2H-1) and Submaximum from 64-100% (p<0.001, 0.30 m*s-2H-1) depth to minimum velocity, respectively (Figure 3b; Table 4).

Table 4. Center of gravity and joint level kinematic ANOVA and post-hoc test results

	Variable	ANOVA (F, loc, p)	Supramax-1RM (Diff, loc, p)	1RM-Submax (Diff, loc, p)	Supramax-Submax (Diff, loc, p)
	COG Velocity (m/s)	8.1, 26-100, <0.001	Not Significant	-0.21±0.15, 36-100, <0.001	-0.19±0.12, 26-100, <0.001
	COG Acceleration (m/s^2)	11.1, 15-27 & 62-100, <0.001	-0.06±0.04, 65-100, <0.001	-0.12±0.10, 14-27, <0.001	-0.05±0.04, 64-100, <0.001
Joint Angles (deg)	Ankle Dr	8.2, 13-84, <0.001	Not Significant	-3.9±2.4, 13-82, <0.001	Not Significant
	Ankle Iv/Ev	8.1, 13-53 & 63-78, <0.004	-4.9±5.4, 67-73, <0.004	3.1±2.7, 13-44, <0.001	Not Significant
	Knee Flx	8.0, 12-100, <0.001	-17.7±13.0, 28-100, <0.001	9.8±4.9, 12-80, <0.001	-15.9±13.6, 72-100, <0.004
	Hip Flx	7.7, 0-100, <0.004	9.5±6.3, 45-100, <0.001	-1.7±2.4, 0-2, <0.004 -3.6±3.1, 12-73, <0.001	7.1±5.2, 62-100, <0.001
	Hip Ad/Abd	7.9, 11-45, <0.004	Not Significant	3.8±3.1, 11-58, <0.001	Not Significant

F, loc, p, and Diff: F-statistic, p-value threshold exceeded, location (percent from depth to minimum velocity), and mean difference ± 1 standard deviation. COG: center of gravity, Dr: dorsiflexion, Iv/Ev: inversion/eversion, Ext: extension, Flx: flexion, Ad: adduction, and Abd: abduction.

Figure 3. Vertical center of gravity velocity and acceleration during the Acceleration and Sticking Regions for Submax, 1RM and Supramax attempts

Figure 3a. ANOVA tests and ensemble vertical center of gravity velocity from depth to minimum velocity.
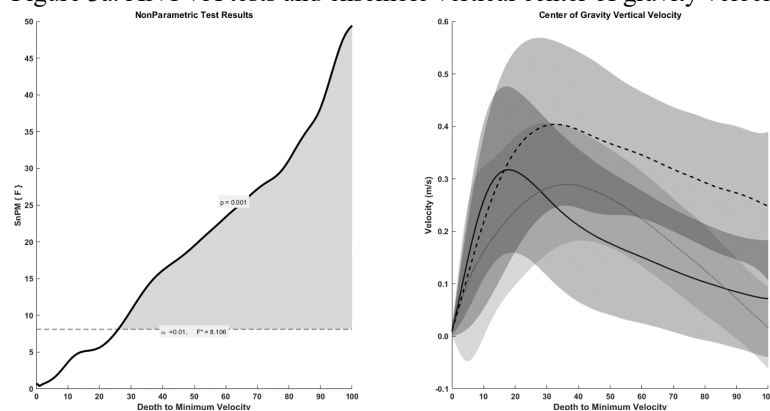
Figure 3b. ANOVA tests and ensemble vertical center of gravity acceleration from depth to minimum velocity.
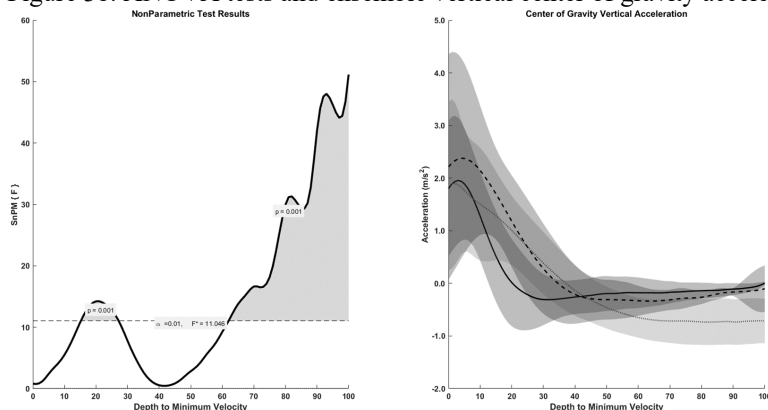
Velocity (2a) and acceleration (2b) ANOVA test results are presented on the left for each figure. Means and one standard deviation are presented on the right for Submax (dashed black line with medium shading), 1RM (black line with dark shading) and Supramax (dotted gray with light shading) attempts. The notation SPM{F} is the test statistic for each ANOVA. The horizontal dotted line is the threshold for statistical significance. Statistically significant test statistics are represented by shaded regions and corresponding p-values. All variables are plotted from depth (minimum point of center of gravity) to minimum center of gravity velocity, encompassing both the Acceleration and Sticking Regions of the back squat.

3.2. Joint Kinematics

1RM had reduced ankle dorsiflexion compared to Submaximum from 13-82% (p<0.001, -3.9 deg.) and reduced ankle eversion compared to Supramaximum from 67-73% (p<0.004, -4.9 deg.) and Submaximum from 13-44% (p<0.001, -3.1 deg.) depth to minimum velocity (Figure 4a; Table 4).

Supramaximum had greater knee flexion compared to 1RM and Submaximum from 28-100% (p<0.001, 17.7 deg.) and 72-100% (p<0.004, 15.9 deg.) depth to minimum velocity (Figure 4b; Table 4). 1RM also had decreased knee flexion compared to Submaximum from 12-80% depth to minimum velocity (p<0.001, -9.8 deg.). No significant differences were found for knee ad/abduction angles.

1RM had reduced hip flexion compared to Supramaximum from 45-100% (p<0.001, -9.5 deg.) and Submaximum from 0-2% (p<0.004, -1.7 deg.) and 12-73% (p<0.001, -3.6 deg.) depth to minimum velocity (Figure 4c; Table 4). It can be difficult to ascertain if a difference less than

3 deg. is meaningful. 1RM also had reduced hip abduction angles compared to Submaximum

from 11-58% depth to minimum velocity (p<0.001, -3.8 deg.; Table 4).

Figure 4. Comparisons of ankle, knee, and hip angles between Submax, 1RM and Supramax attempts
Figure 4a. ANOVA tests and ensemble ankle angles from depth to minimum velocity.
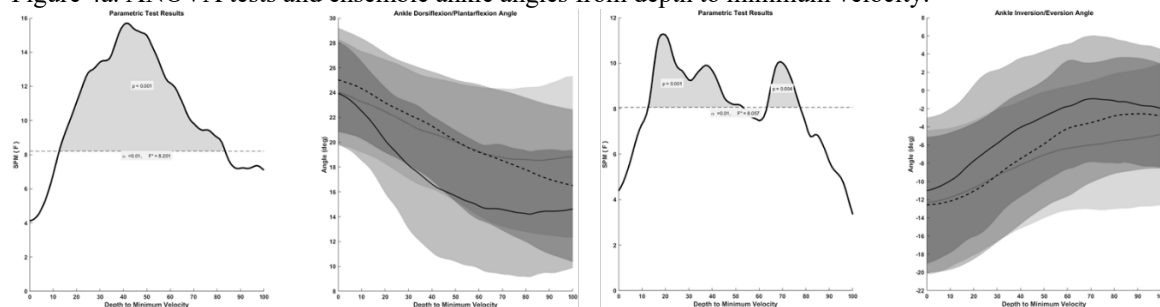
Figure 4b. ANOVA tests and ensemble knee angles from depth to minimum velocity.
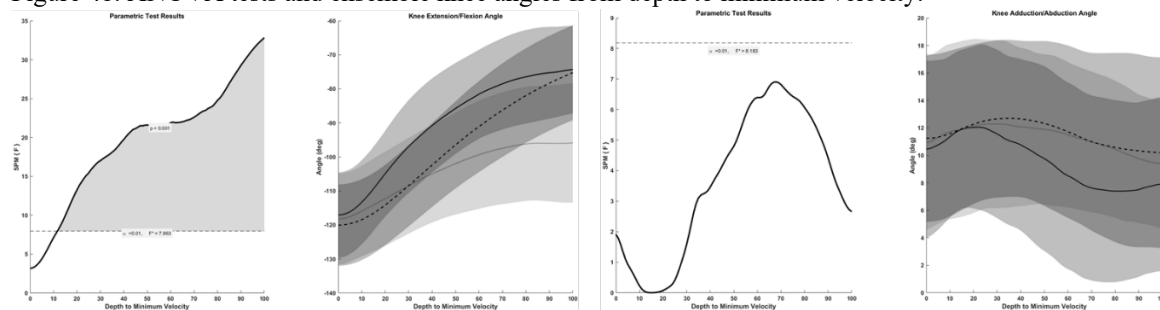
Figure 4c. ANOVA tests and ensemble hip angles from depth to minimum velocity.
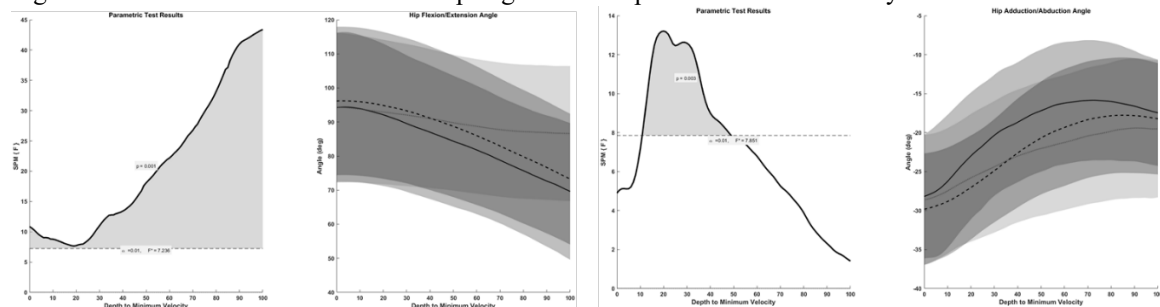
Figures a-c present sagittal plane and frontal plane ankle (4a), knee (4b), and hip (4c) test results and ensemble data. SPM{F} is the test statistic. The notation SPM{F} is the test statistic for each ANOVA. The dotted line is the threshold for statistical significance. Statistically significant test statistics are represented by shaded regions and corresponding p-values. Means and one standard deviation are presented for Submax (dashed black line with medium shading), 1RM (black line with dark shading) and Supramax (dotted gray with light shading) attempts. All variables are plotted from depth (minimum point of center of gravity) to minimum center of gravity velocity, encompassing both the Acceleration and Sticking Regions of the back squat.

3.2. Joint Kinetics

1RM had increased ankle eversion moments compared to Supramaximum from 67-70%

(p<0.004, 0.10 Nm/kg) and Submaximum from 40-41% and 47-59% (p<0.004, 0.07 Nm/kg &

p<0.001, 0.08 Nm/kg) depth to minimum velocity (Figure 5b, Table 5). Supramaximum had increased knee extension moments compared to 1RM from 15-53% (p<0.001, 0.31 Nm/kg) and 63-79% (p<0.001, 0.27 Nm/kg) and Submaximum from 40-60% (0.22 Nm/kg), 68-82% (0.21 Nm/kg), and 90-97% (0.25 Nm/kg) (all p<0.001) depth to minimum velocity (Figure 6a; Table 5). Submaximum had reduced hip extension moments compared to 1RM from 20-100% (p<0.001, -0.41 Nm/kg) and Supramaximum from 0-11% (p<0.004, -0.34 Nm/kg) and 82-100% (p<0.001, -0.44 Nm/kg) depth to minimum velocity (Figure 7a; Table 5). Submaximum also had increased hip abduction moments compared to Supramaximum from 82-100% (p<0.001, 0.28 Nm/kg) depth to minimum velocity (Figure 7b; Table 5).

Table 5. Joint moment ANOVA and post-hoc test results

	Variable	ANOVA (F, loc, p)	Supramax-1RM (Diff, loc, p)	1RM-Submax (Diff, loc, p)	Supramax-Submax (Diff, loc, p)
Moments (Nm/BM)	Ankle In/Ev	8.5, 39-80, <0.004	0.10±0.10, 67-70, <0.004	-0.07±0.07, 40-41, <0.004 -0.08±0.07, 47-59, <0.001	Not Significant
	Knee Ext	8.8, 16-82, <0.001 8.8, 90-97, <0.004	0.31±0.33, 15-53, <0.001 0.27±0.30, 63-79, <0.001	Not Significant	0.22±0.26, 40-60, <0.001 0.21±0.25, 68-82, <0.001 0.25±0.25, 90-97, <0.001
	Knee Ad/Abd	8.7, 80-100, <0.004	Not Significant	Not Significant	0.23±0.23, <0.001, 82-100
	Hip Ext	9.7, 0-100, <0.001	Not Significant	-0.41±0.21, 20-100, <0.001	-0.34±0.26, 0-11, <0.004 -0.44±0.21, 14-100, <0.004
	Hip Ad/Abd	8.5, 42-100, <0.001	Not Significant	Not Significant	0.28±0.25, 82-100, <0.001
Support Moment (%)	Knee Contribution	9.0, 12-30, <0.004	3.9±3.4, 13-25, <0.001	-3.1±3.1, <0.004, 16-25	Not Significant
	Hip Contribution	8.9, 9-34, <0.001 8.9, 57-74, <0.004	-4.3±3.4, 9-27, <0.001	2.8±2.1, 13-32, <0.001 4.6±4.1, 57-72, <0.001	Not Significant

Moments are internal, normalized to body mass (BM), and follow right hand rule. F, loc, p, and Diff: F-statistic, p-value threshold exceeded, location (percent from depth to minimum velocity), and mean difference ± 1 standard deviation. In/Ev: inversion/eversion, Ext: extension, Flx: flexion, Ad/Abd adduction/abduction.

Figure 5. Comparisons of sagittal and frontal plane ankle moments between Submax, 1RM and Supramax attempts

Figure 5a. Sagittal plane ankle moments normalized to body mass.
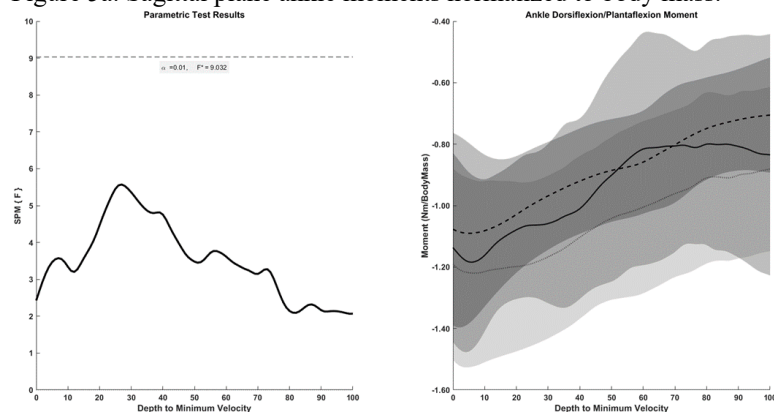
Figure 5b. Frontal plane ankle moments normalized to body mass.
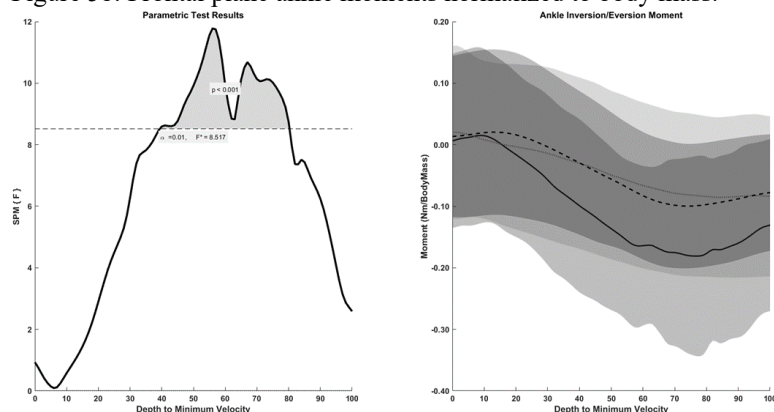
Figures a & b present ANOVA test results (left columns) and ensemble data for sagittal plane (4a) and frontal plane (4b) ankle moments normalized to body mass (right columns). SPM{F} is the test statistic. The notation SPM{F} is the test statistic for each ANOVA. The dotted line is the threshold for statistical significance. Statistically significant test statistics are represented by shaded regions and corresponding p-values. Means and one standard deviation are presented for Submax (dashed black line with medium shading), 1RM (black line with dark shading) and Supramax (dotted gray with light shading) attempts. All variables are plotted from depth (minimum point of center of gravity) to minimum center of gravity velocity, encompassing both the Acceleration and Sticking Regions of the back squat.

Figure 6. Comparisons of sagittal and frontal plane knee moments between Submax, 1RM and Supramax attempts

Figure 6a. Sagittal plane knee moments normalized to body mass.
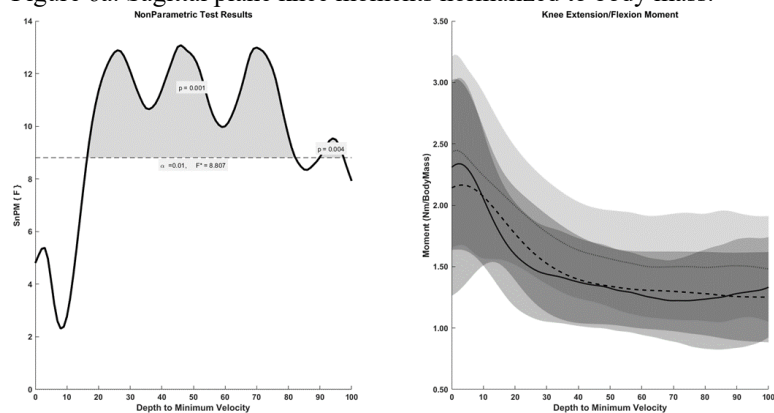
Figure 6b. Frontal plane knee moments normalized to body mass.
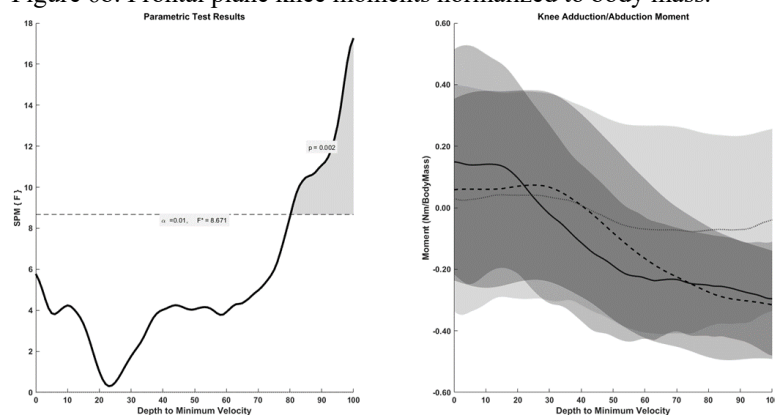
Figures a & b present ANOVA test results (left columns) and ensemble data for sagittal plane (5a) and frontal plane (5b) knee moments normalized to body mass (right columns). SPM{F} is the test statistic. The notation SPM{F} is the test statistic for each ANOVA. The dotted line is the threshold for statistical significance. Statistically significant test statistics are represented by shaded regions and corresponding p-values. Means and one standard deviation are presented for Submax (dashed black line with medium shading), 1RM (black line with dark shading) and Supramax (dotted gray with light shading) attempts. All variables are plotted from depth (minimum point of center of gravity) to minimum center of gravity velocity, encompassing both the Acceleration and Sticking Regions of the back squat.

Figure 7. Comparisons of sagittal and frontal plane hip moments between Submax, 1RM and Supramax attempts

Figure 7a. Sagittal plane hip moments normalized body mass.
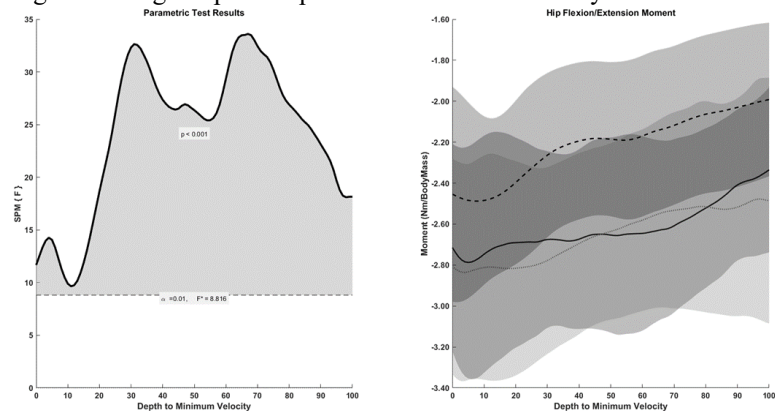
Figure 7b. Frontal plane hip moments normalized to body mass.
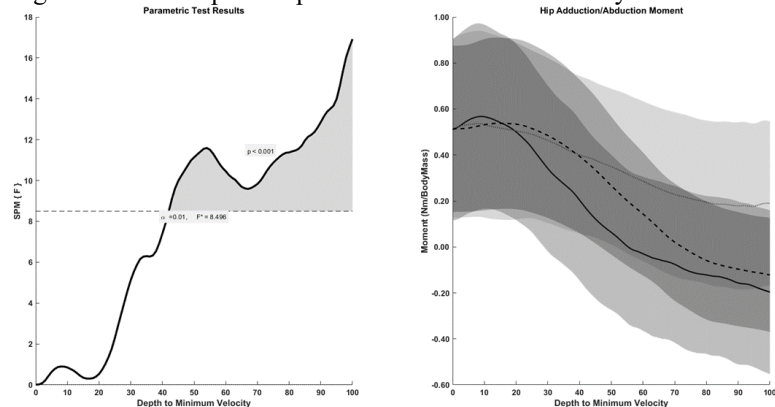
Figures a & b present ANOVA test results (left columns) and ensemble data for sagittal plane (5a) and frontal plane (5b) hip moments normalized to body mass (right columns). SPM{F} is the test statistic. The notation SPM{F} is

the test statistic for each ANOVA. The dotted line is the threshold for statistical significance. Statistically significant test statistics are represented by shaded regions and corresponding p-values. Means and one standard deviation are presented for Submax (dashed black line with medium shading), 1RM (black line with dark shading) and Supramax (dotted gray with light shading) attempts. All variables are plotted from depth (minimum point of center of gravity) to minimum center of gravity velocity, encompassing both the Acceleration and Sticking Regions of the back squat.

1RM had reduced contributions from the knee to the support moment compared to Supramaximum from 13-25% (p<0.001, -3.9%) and Submaximum from 16-25% (p<0.004, -3.1%) depth to minimum velocity (Figure 8; Table 5). 1RM also had increased contributions from the hip compared to Supramaximum from 9-27% (p<0.001, 4.3% increase) and Submaximum from 13-32% (p<0.001, 2.8% increase) and 57-72% (p<0.001, 4.6% increase) depth to minimum velocity (Figure 8; Table 5).

Figure 8. Comparisons of the support moment and joint contributions to the moment
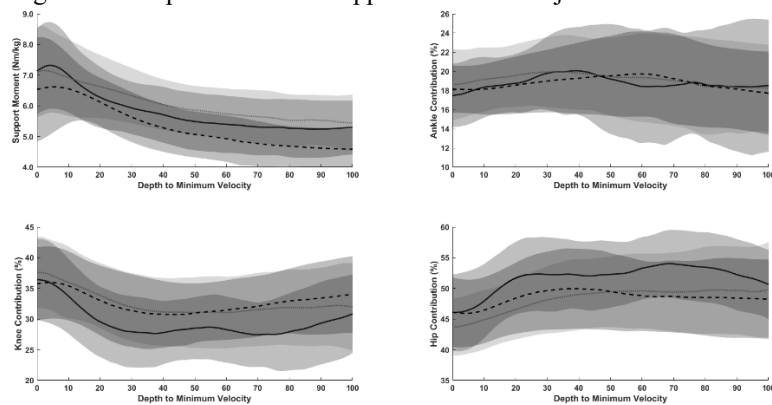
The support moment was derived as the sum of sagittal and frontal plane hip, knee, and ankle moments and normalized to body mass. Ankle, knee, and hip contributions were derived as the percentage of their summed sagittal and frontal plane moments against the support moment. Means and one standard deviation are presented for Submax (dashed black line with medium shading), 1RM (black line with dark shading) and Supramax (dotted gray with light shading) attempts.

4. Discussion

The purpose of this study was to determine the effects of loading on performance and lower extremity biomechanics during the acceleration and sticking region of back squats. Our first hypothesis was only partially supported as a greater knee to hip transition was found for 1RM, but not Submaximum, squats compared to Supramaximum squats. In addition, differences in knee and hip moments between Supramaximum and 1RM/Submaximum did not occur at similar timings. Our second hypothesis, increased vertical velocity and accelerations, was only

partially supported as well. Increased vertical velocity was present for Submaximum squats compared to both 1RM and Supramaximum, but not between 1RM and Supramaximum squats. Increased accelerations for 1RM and Submaximum only occurred during late sticking region.

Previous research has implemented vertical velocity as a discriminative measure for performance (Elliott et al., 1989; Escamilla, Fleisig, Lowry, et al., 2001; Kompf & Arandjelović, 2016, 2017; Orjalo et al., 2017; van den Tillaar, 2015) especially for the sticking region. However, this study found vertical velocity was only different between Submaximum and the heavier loaded conditions. The lack of differences in vertical velocity between the Supramaximum and 1RM squats could indicate that failure lifting loads beyond 1RM may not actually be evident until after the sticking region. However, in contrast to vertical velocity, vertical accelerations were significantly different between all levels of loading during the sticking region. The higher order kinematic variable demonstrates that although vertical velocity may be maintained at similar levels in Supramaximum compared to 1RM squats, failure in the Supramaximum squats begins midway through the sticking region. Therefore, we pose that vertical acceleration is a more definitive measure of performance in back squats than the ever popular vertical velocity.

The joint-level kinematic and kinetic waveforms presented here provide insight into how lower mechanics relate to whole-body kinematics across acceleration and sticking regions. First, the knee moment mirrors vertical COG acceleration, with both waveforms presenting an early peak and a sharp decline leading up to peak velocity (Figures 3a-b and 6a). Similar to our results, previous research has found knee extensor moments were largest at full depth and during the initial portion of the ascent (depth to 90° knee flexion) and declined thereafter (Escamilla, Fleisig, Lowry, et al., 2001; Flanagan et al., 2003). Second, there is a decline in the knee joint

contributions (summed sagittal and frontal plane moments) to the support moment during the sticking region, whereas hip moment contributions increase (Figure 8). The knee and hip biomechanics waveforms indicate a transition from early emphasis on knee loading during acceleration to hip loading during the sticking region (Figures 6a, 7a, & 8). A knee-hip transition was suggested previously by van den Tillaar, who postulated that a transition from an emphasis on knee extensors to the gluteus maximus is responsible for a successful exit of the sticking region (van den Tillaar, 2015). In addition, previous research found hip loading generally constant from full depth to minimum bar velocity (same as the depth to minimum velocity within the current study), while knee loading decreased (Escamilla, Fleisig, Lowry, et al., 2001). Lastly, while ankle contributions are much lower than knee and hip (Flanagan et al., 2003), the ankle moments provided a near constant 15-20% of the support moment during all squats (Figure 8). Thus, some focus on plantaflexor strength and ankle mobility is warranted for training programmes. Considering the popularity of weight-lifting shoes with raised heels (generally worn to circumvent limited ankle mobility), future work should also analyse how shoe heel size can affect contributions of the ankle plantarflexors during maximal back squats.

The effects of load were not consistant across lower extremity biomechanics. However, there are aspects that can enhance our understanding of the relationship between load and squat mechanics. First, differences in joint-level kinematics appear earlier than performance variables (velocity and acceleration) and occur across both acceleration and sticking regions. In particular, 1RM squats were performed with increased knee extension motion compared to both Supramaximun and Submaximum squats within the acceleration region, along with increased sagittal and frontal plane motion compared to Submaximum squats for large portions of the acceleration region. Both 1RM and Submaximum squats had increased knee and hip extension

motion during the latter portion of the sticking region. Based on these kinematic results, 1RM squats were performed by implementing quicker simultaneous knee and hip extension when accelerating out of full depth, thus reaching peak velocity earlier than both Submaximum and Supramaximum squats. In contrast, participants appear to be unable to reach a similar explosion from full depth when the resistance (barbell load) was beyond maximum strength. Thus, supramaximum squats maintained similar kinematic waveforms, albeit muted, to Submaximum squats throughout most of the acceleration and sticking regions. Second, our results illustrate that submaximum squats performed at a higher velocity than 1RM squats and place similar loads on the ankle and knee extensors, but reduced loads on the hip extensors. Therefore, training back squats at a submaximal level to full depth could be efficient alternatives to maximal training for knee and ankle loading (Duncan et al., 2014; Eslava et al., 2006; Marshall et al., 2011; Sanborn et al., 2000; van den Tillaar, 2015). However, the significantly greater loading on the hip extensors/adductors that occurs with increased resistance suggests heavier loading schemes may be required for hip training emphasizing hip musculature (M. Bryanton et al., 2012; M. A. Bryanton et al., 2015; Flanagan & Salem, 2008; Yavuz et al., 2015).

This study also provides some reasoning behind failure when small increases beyond maximal strength (Supramaximums were at 105% 1RM) are applied during back squats. Supramaximum squats were performed with greater knee loading compared to both 1RM and Submaximum squats, along with greater hip loading compared to Submax squats. Similar to increased velocity, some differences should be expected due to an increase in external resistance (barbell mass). However, Supramaximum squats were also performed with a greater emphasis on knee and reduced emphasis on hip loading compared to 1RM squats. To date, only one previous study has evaluated failed versus successful maximum back squat kinematics (Flanagan et al.,

2015). The previous report found that success during back squats is dependent upon hip loading, but could also be subject-specific (Flanagan et al., 2015). Although the previous report implemented muscular fatigue to induce failure (i.e. repeated reps at the same weight) and did not compare across different loads (Flanagan et al., 2015), similarities exist between their results and the current study. Importantly, despite differences in methodology, the previous work and our current study demonstrate joint-level biomechanics appear to be more descriptive of squat performance than whole-body kinematics (i.e. velocity/acceleration). In addition, these results indicate sufficient strength and emphasis on hip musculature is an integral factor for successfully lifting heavy (maximal/supramaximal) loads during back squats.

5. Conclusions

This study aimed to increase our understanding of the sticking region's relationship with success and failure of maximally loaded back squats. We identified three important factors for successful maximal back squats; 1) contrary to the focus from previous literature, vertical acceleration is a greater discriminatory measure than velocity for back squats. 2) Submaximum squats performed at increased velocities can elicit similar ankle and knee contributions as maximal squats. Thus, submaximal loaded squats are an alternative to maximal training, but not for training the hip. 3) Finally, considering the large moments and contributions found at the hip joint, hip strength throughout the range of motion of a squat needs to be emphasized.

6. Limitations

There are several limitations to acknowledge in this study. Males and females were combined in this study; thus, future studies could evaluate males and females separately as anthropometric differences often exist between sexes. This study would be improved upon with a larger subject pool. The subjects were resistance trained, but not necessarily elite level; thus,

squat form and techniques could be variable between levels of training. The transverse plane data was not included in this study as the sagittal and frontal planes accounted for a majority of the joint moments and motions. A future study could include all three planes of motion to further elucidate the differences between failed and successful back squat attempts. Other studies have found foot placement and squat depth influence weight lifted, vertical velocity, and joint moments (Caterisano et al., 2002; Escamilla, Fleisig, Lowry, et al., 2001; Hammond et al., 2016; Jaberzadeh et al., 2016). Thus, future work in this area may also consider allowing athletes to perform squats with their own form. The warmup was not standardized as a specific and dynamic warmup is going to be unique to each athlete's requirements.

CHAPTER 3. EVIDENCE FOR THE USE OF DYNAMIC MAXIMUM NORMALIZATION METHOD OF MUSCLE ACTIVATION DURING WEIGHTED BACK SQUATS

Abstract

Electromyography (EMG) is a popular technique for analyzing muscle activation profiles during athletic maneuvers such as the back squat. Two methods are commonly implemented for normalizing EMG: a maximum voluntary isometric contraction (MVIC) and a dynamic maximum during the task being performed (DMVC). Although recent literature suggests DMVC may be superior, these suggestions haven't been examined for weighted exercises. This study examined the influence of normalization method on rectus femoris, vastus medialis, and biceps femoris activations during back squats. Muscle activations were collected on twenty-seven participants (13 females, 14 males) performing one-repetition maximum (DMVC) and submaximum (80%) back squats. Data from submaximum squats were normalized to MVICs and DMVC. Data were compared using intra-class correlations over two testing days, variance ratio, and coefficients of variation. Mixed-model ANOVAs were used to elucidate the influence on intra-participant (method) and inter- (sex) subject variability (method). Reliability was "good" or "excellent" for MVIC and "excellent" for DMVC. Inter-subject variability was greater for MVIC compared to DMVC for all muscles. A significant normalization by sex interaction for both peak and mean biceps femoris activation was found. Based on our findings and current literature, normalization to DMVC is the superior method for weighted exercises.

1. **Introduction**

The squat is a multi-joint and multi-planar exercise that requires activation from all lower extremity muscles in some capacity (Yavuz et al., 2015). The squat is a cornerstone exercise for

athletic strength training programs and has been extensively researched. Electromyography (EMG) is one of the most frequently used analyses in squat research. EMG has been used to determine the most advantageous movement patterns for maximum muscle activation (Contreras et al., 2015), to address muscle contributions to patellofemoral pain syndrome (Nakagawa et al., 2012), to evaluate alternate weighted movements to decrease knee loading (Lynn & Noffal, 2012), and to assess altering lower extremity joint alignment and squat depths (Jaberzadeh et al., 2016). Several studies have also evaluated muscle activation during squatting to different depths, with different weights lifted, and with different foot placement (Balshaw & Hunter, 2012; Escamilla, Fleisig, Lowry, et al., 2001; Murray et al., 2013).

Muscle activation is typically reported as a normalized EMG signal. Many factors influence the resultant EMG signal amplitude (i.e. extrinsic (electrode specific characteristics), intrinsic (muscle specific characteristics)) that can be neutralized with normalization (De Luca, 1997). Furthermore, normalizing EMG signals can improve within-group homogeneity, allowing for differences between groups to be more easily detectable (A. Burden, 2010). Utilization of non-normalized EMG data should be avoided (Besomi et al., 2020). Several methods for obtaining a reference value can be used (Besomi et al., 2020), the most common of which is the maximum voluntary isometric contraction (MVIC). However, the Consensus for Experimental Design in Electromyography (CEDE) project recently put forth guidelines stating MVIC and/or non-normalized EMG are cautioned against if the tasks being evaluated are different than the maneuver performed for the reference collection (Besomi et al., 2020).

In contrast to MVIC, EMG can be normalized to the peak EMG signal of the dynamic task being performed (Balshaw & Hunter, 2012). In fact, the first use of normalization of an EMG signal evaluated the signal as a percentage of the maximal activity during the task being

recorded (Eberhart et al., 1954). Dynamic movements demonstrate greater muscle activations that are characterized by a higher peak in EMG amplitude than those found in MVIC trials (Ricard et al., 2005; Suydam et al., 2017). A previous EMG analysis also found muscle activation is greatest in lower extremity muscles during the ascending phase of the back squat (Gullett et al., 2009), which is notably the time when lift failure can occur. Although previous EMG research is quite extensive on back squats, there are important methodological factors to consider when culminating the literature on muscle activation patterns during dynamic maneuvers. In unconstrained ballistic tasks, peak EMG of the ballistic task produces greater within-participant variability, computed as the intraclass correlation coefficients (ICC) for each muscle, than peak EMG of the MVIC trials (Suydam et al., 2017). In addition to intraclass correlation coefficients, the coefficient of variation (CV) and variance ratio (VR) (Hershler & Milner, 1978) techniques are useful measures to analyze datasets. Using CV and VR, several studies have found support for (Allison et al., 1993; A. Burden & Bartlett, 1999; A. M. Burden et al., 2003; Chapman et al., 2010; Kashiwagi et al., 1995; Knutson et al., 1994; Yang & Winter, 1984) and against (Bolgla & Uhl, 2007) the usage of a dynamic maximum for normalization.

Maximal loading is required for full activation of muscles (Yavuz et al., 2015) which could suggest the use of a dynamic maximum voluntary contraction (DMVC) is a more applicable normalization technique than MVIC for EMG signals during weighted exercise movements (Besomi et al., 2020). In agreement, Balshaw and Hunter (2012) found normalizing to a submaximum dynamic squat trial demonstrated greater absolute reliability for both the vastus lateralis and the biceps femoris compared to MVIC trials when analyzing back squats. Further studies conducted on lower extremity musculature in non-squat studies also found normalizing to a dynamic trial is a more reliable normalization technique (Albertus-Kajee et al.,

2011; Clarys, 2000; Suydam et al., 2017). Additionally, the comparison of EMG signals collected at different muscle lengths and contraction speeds (such as the differences between a dynamic movement and an isometric measurement) is not recommended (Vigotsky et al., 2018). However, there are methodological considerations regarding dynamic maximums: 1) small modifications in technique could alter activations from expected norms/previous assessments, 2) not all dynamic tasks will adequately maximize muscle activation (e.g., abdominal activation during jump vs. sit-up), and 3) repeating dynamic maximums (e.g., for each of several days of data collection) could be taxing, thus extended rest periods would be required compared to MVICs. Consideration of normalization procedure is also crucial for between-participants' comparisons, as the normalization scheme, which should inherently reduce inter-participant variability, will affect group-based comparisons.

The back squat presents a unique opportunity to simultaneously evaluate intra (normalization method) and inter (group) participant effects due to 1) the similarity in joint angles during the squat and MVIC setup and 2) the presence of back squats in nearly all exercise program for all persons (males and females). Currently, there is no universally adopted method for normalization of muscle activation during weighted exercises, likely due to the mixed results from previous comparisons between each scheme. As such, research studies analyzing the advantages and disadvantages of each normalization scheme are warranted. The purpose of this study was to evaluate the effects of MVIC and dynamic maximum normalization methods on intra- and inter- group variability and reliability of muscle activity during weighted back squats. This study includes an inter-group (sex) comparison to illustrate the importance of normalization method when analyzing weighted back squats.

2. Methods

2.1. Participants

This study was approved by the University Institutional Review Board. The design of the study included power analysis using G*Power (version 3.1.9.6) with an alpha level of 0.05 and a power of 0.80. As there were no existing data in the literature, interaction effect power analyses were based on a "medium" effect size (0.25) and indicated a minimum total sample of 28 was required. Power analyses on sex main effects were performed using data from multiple studies ((Mehls et al., 2020), effect size 1.18; (Lynn & Noffal, 2012), effect size 0.85; (Zeller et al., 2003), effect size 2.0), indicating a minimum of 18 participants (9 male/9 female) were required. Power analyses for normalization main effects using existing literature ((Suydam et al., 2017); study effect size 1.17) indicated a minimum of 11 participants were required. Twenty-seven adults were recruited from the surrounding area using flyers (Table 6). To take part in the study, participants were required to be 18-55 years, have no history of knee injuries, and perform weighted back squats at or near maximum loads at least once a week for the past year. Participants were excluded from the study if they had any major lower extremity injuries in the past 3 months, experienced any knee pain in the past 6 months, any diagnosis of lower extremity joint arthritis, or a body mass index greater than 35 kg/m2. All participants signed informed consent forms.

Table 6. Participant demographics

	N	Age (years)	Mass (kg)	Height (m)	BMI (kgm^{-2})
Female	13	26.5±5.4	73.03±15.08	1.63±0.05	26.45±4.62
Male	14	26.2±3.4	84.46±9.88	1.77±0.07	26.46±2.83

Notes: N - number of participants per group. BMI - body mass index.

2.2. MVIC Collection Procedures

MVICs of each muscle were recorded for 10 seconds pulling against resistance from a strap securely attached to the wall. Familiarization was ensured for each test prior to recording

the MVIC. First the procedures were explained verbally, then the participant performed several practice MVIC tests, not to include maximum exertion. Once the participant indicated they were comfortable with the testing procedures, at least two MVICs were collected for each muscle group, with a 2-minute rest period between tests. The RF and VM MVIC test was performed seated with the knees flexed 60° (Barbero et al., 2012; Konrad, 2006). The BF MVIC was performed prone with the knee flexed to 30° (Barbero et al., 2012; Konrad, 2006).

2.3. DMVC Collection Procedures

Reflective markers were placed bilaterally on anatomical landmarks (acromion processes, iliac crests, anterior and posterior superior iliac spines, greater trochanters, medial and lateral femoral epicondyles, medial and lateral malleoli, and 1st and 5th metatarsal heads). Additional clusters of four tracking markers attached to rigid plastic shells were secured to the shoe heels, and lateral thighs and shanks (Maddox et al., 2020).

Prior to beginning the 1RM testing, participants were allowed five minutes for warming up and stretching of their choice. Participants were instructed to squat with shoulder-width stance and descend to full depth (contact between posterior thigh and shank). Knee flexion angles attained through the full depth squat were ~120° (Maddox et al., 2020), which is in full agreement with previous research (M. Bryanton et al., 2012; Endo et al., 2020; Y. Lu et al., 2020; Marchetti et al., 2016). "Bouncing" out of the bottom of the squat was not permitted and was regulated by a command of, "one, up," when full depth was achieved. Participants were not permitted to wear any other gear (weightlifting shoes, belts, etc.). Spotters were used on each side of the participant during all lifts. Participants were directed to avoid any lower body resistance training for 48-hours before the session. Next, participants completed the NSCA's 1RM testing protocol (Haff & Triplett, 2016). Participants were given 20 minutes to warm up to

their 1RM. After completion of the 1RM protocol and a subsequent rest period of at least 10 minutes, participants performed a back squat with 80% of their 1RM.

Fifteen participants performed a follow up testing session 5-7 days later, after confirming soreness/residual fatigue had fully dissipated. The focal point of these data are reliability analyses.

2.4. Data Processing Procedures

Muscle activation patterns were collected at 2000 Hz using a Delsys Trigno Wireless EMG system (Delsys, Inc.) with electrodes that were single differential, pre-amplified by a factor of 1000, composed of 99.9% silver, had a contact area of 5 mm^2 perpendicular to the electrode orientation, with an inter-electrode distance of 10 mm. The electrode diameter and inter-electrode distance satisfy the Nyquist-Shannon sampling criterion (Merletti & Muceli, 2019). The skin above the palpated muscle bellies of the rectus femoris (RF; midpoint of ASIS to patella), vastus medialis (VM; 80% of distance between ASIS and medial collateral ligament), and biceps femoris long head (BF; midpoint of ischial tuberosity to lateral epicondyle) (Barbero et al., 2012) were prepped by shaving (if hairy), abrading using sanding pads, and cleaning with alcohol wipes. EMG electrodes were then placed on the skin above the muscle bellies and oriented such that the silver bar contacts were perpendicular to the muscle fiber, according to Surface ElectroMyoGraphy for the Non-Invasive Assessment of Muscles (SENIAM), the Consensus for Experimental Design in Electromyography (CEDE), and Delsys Trigno guidelines.

2.5. Data Analysis

Recorded muscle activations from MVIC, 1RM (DMVC) and 80% 1RM (submax) trials were imported into MATLAB (R2019b, The MathWorks, Natick, MA). EMG waveforms during

the concentric phase (from full depth to standing upright; (Maddox et al., 2020)) were used for analyses. The concentric phase was chosen as it required the greatest activations of all recorded muscles, which has also been found in previous literature (Gullett et al., 2009; Yavuz et al., 2015). The muscle activation signals were high-pass filtered at 20 Hz and full-wave rectified (De Luca et al., 2010). Residual analyses were performed on the rectified signal, which indicated the optimal low-pass frequency cutoff was 5 Hz across all muscles. Thus, the rectified signal was low pass filtered at 5 Hz using a 4th order Butterworth filter.

In agreement with the guidelines presented by CEDE, the peak signals from the DMVC and MVIC were extracted and used for normalization (Besomi et al., 2020). To minimize transient peaks as the normalization value, the MVIC and DMVC waveforms were subdivided into 20-frame windows (0.01s) and averaged within windows. Peak MVIC and DMVC signals were recorded as the peak window. All submax trials were normalized to MVIC and DMVC. Peak activation signals during submax trials were determined in the same manner as above. In addition to peak activation, mean muscle activation during the submax trials were also computed. Mean activation was derived by dividing the area under the activation-time waveform (using trapezoid integration function in MATLAB) by time of the concentric phase. Both peak and mean activation signals were normalized to DMVC and MVIC for comparisons. Mean knee and hip joint angles at timing of peak activation in all three planes for each of the muscles were extracted and are provided (Table 7).

Table 7. Joint positions at maximum EMG: mean±std

	80% 1RM			1RM - DMVC		
	RF	VL	BF	RF	VL	BF
Sagittal						
Knee	-105.8±24.6°	-89.4±22.9°	-68.8±19.3°	-96.2±20.6°	-85.7±15.4°	-66.2±12.7°
Hip	90.9±24.6°	78.0±23.6°	63.3±22.6°	88.0±20.9°	82.7±18.8°	59.6±16.1°
Frontal						
Knee	11.2±6.7°	10.8±7.1°	8.0±5.5°	10.1±5.3°	10.1±6.2°	5.6±5.6°
Hip	-25.1±8.5°	-22.6±8.1°	-18.5±6.9°	-20.1±9.2°	-18.6±8.4°	-17.5±7.9°
Transverse						
Knee	9.8±11.1°	4.7±10.8°	0.3±7.6°	2.9±10.4°	0.1±7.9°	-0.6±6.7°
Hip	12.3±9.8°	5.7±11.4°	-2.3±9.6°	10.2±7.4°	7.6±7.2°	-3.0±7.7°

Note: DMVC: dynamic maximum voluntary contraction during 1-RM; RF: rectus femoris; VM: vastus medialis; BF: biceps femoris long head. Maximum voluntary isometric contractions for RF and VM were collected seated with hip at 90° and knee at 60°; BF MVICs were collected prone with hip at 0° and knee at 30°.

Inter-participant variability for both normalization techniques was assessed with CV and VR (Yang & Winter, 1984). Test-retest (sessions 1 and 2) reliability was assessed by ICCs (Balshaw & Hunter, 2012) on the fifteen participants that completed two testing sessions.

2.6. Statistical Measures

All data were imported into SPSS Statistics for Windows (version 26.0, IBM Corp.). Reliability of MVIC and DMVC peak values obtained across the two testing sessions was determined using two-way mixed model ICC. F-statistic ($F_{(14,14)}$), p-values, and ICC-statistics are reported for each muscle and normalization method. ICCs were defined as poor (ICC < 0.40), fair (0.40 to 0.60), good (0.60 to 0.75), and excellent (0.75 to 1.00) (Portney & Watkins, 2000).

Normality was assessed for all normalization method/sex variables using Shapiro-Wilk statistics. Variables with normality issues were first investigated for outliers/influential datapoints. Two variables required transformation to fit the normality assumptions for statistical testing. Due to their positive skew distributions, peak BF and VM activations were transformed using the common logarithm. No variables required non-parametric tests due to persistent normality issues. Mixed-model analyses of variance were performed to determine if significant normalization (within-participants; n=2) by sex (between-participants; n=2) interactions existed for each muscle. F-statistics and partial eta-squared values are reported for interaction and main effects. Post hoc tests (in the presence of an interaction) were performed using studentized tests. The Benjamini-Hochberg procedure was used to control for multiple comparisons with a false-discovery rate of 10% (Benjamini & Hochberg, 1995). Ten tests were included in determining the critical threshold for interactions (ANOVAs plus post hoc tests). Six tests were included for

main effect comparisons. Cohen's D effect sizes of sex comparisons for each muscle are also

provided to further elucidate discrepancies between normalization methods.

3. Results

3.1. Reliability & Intra-participant Variability

Results for ICCs analyses can be found in Table 8. Reliability levels were excellent for

RF (ICC: 0.78), VM (ICC: 0.82), and BF (ICC: 0.82) for DMVC across testing sessions.

Reliability levels were good for RF (ICC: 0.74) and VM (ICC: 0.67) and excellent for BF (ICC:

0.80) during MVIC across testing sessions.

Table 8. Reliability statistics for both MVIC and DMVC tests measured across two testing sessions

	MVIC				DMVC			
	F-Stat	p-value	ICC (95% Low-Upp)	Differences Mean±SE	F-Stat	p-value	ICC (Low-Upp)	Differences Mean±SE
RF	6.765	0.001	0.735 (0.374-0.905)	-0.138±0.102	7.548	<0.001	0.776 (0.435-0.922)	-0.053±0.109
VM	4.914	0.004	0.660 (0.238-0.875)	0.134±0.151	9.802	<0.001	0.820 (0.535-0.938)	-0.118±0.169
BF	8.231	<0.001	0.795 (0.469-0.930)	-0.385±0.192	9.695	<0.001	0.822 (0.533-0.939)	-0.044±0.096

Note: Intraclass correlations were performed on the peak values measured on two sessions separated by 5-7 days; MVIC: maximum voluntary isometric contraction, DMVC: dynamic maximum voluntary contraction during 1-RM; RF: rectus femoris; VM: vastus medialis; BF: biceps femoris long head; F-Stat, ICC, and Low-Upp: F-test statistic (14, 14), intraclass correlation statistic, and lower-upper bounds of 95% confidence interval, respectively. Mean differences (between sessions) and standard error (SE) reported are normalized to peak activation obtained from session 1.

Results for variability can be found in Figure 9. RF VR, peak CV, and mean CV were

0.68, 0.51, and 0.42 for MVIC and 0.51, 0.27, and 0.27 for DMVC. VM VR, peak CV, and mean

CV were 0.91, 0.74, and 0.66 for MVIC and 0.63, 0.41, and 0.20 for DMVC. BF VR, peak CV,

and mean CV were 0.93, 0.94, and 0.79 for MVIC and 0.78, 0.46, and 0.36 for DMVC.

Figure 9. Ensemble muscle activation waveforms and inter-subject variability
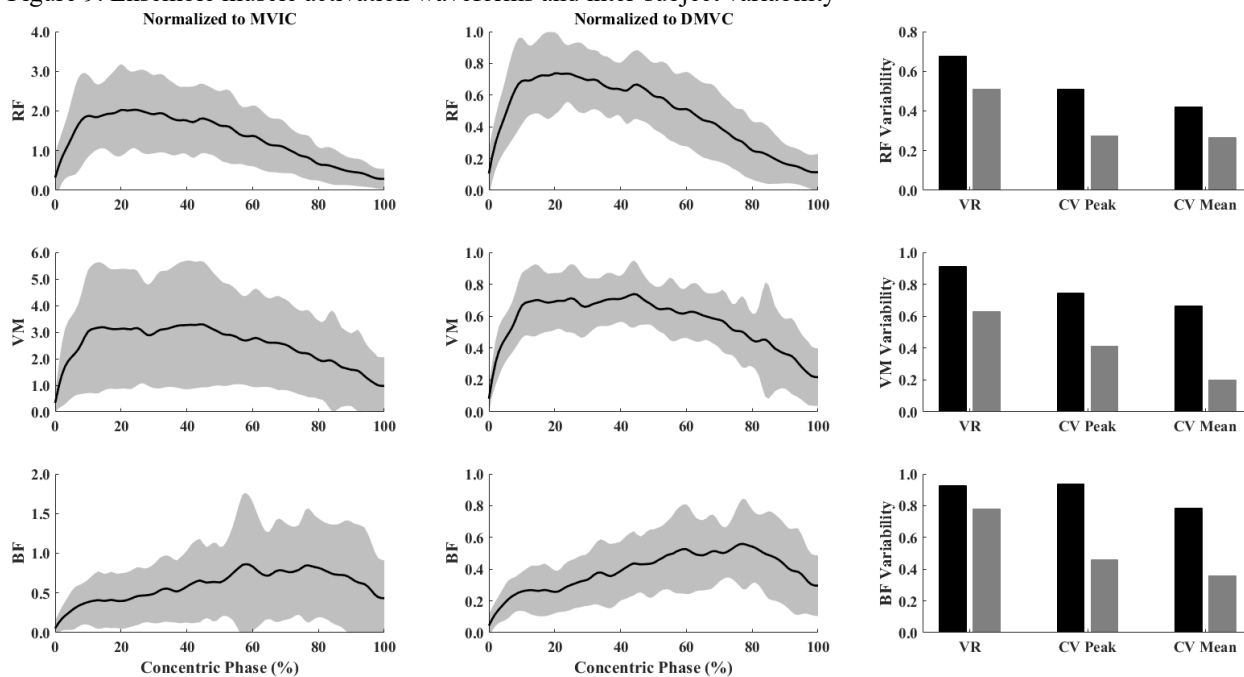
Ensemble rectus femoris (RF; top row), vastus medialis (VM; middle row), and biceps femoris long head (BF; bottom row) mean (lines) and 1-standard deviation (shading) muscle activations during the concentric phase of back squats normalized to maximum voluntary isometric contractions (MVIC) and dynamic maximum contractions (DMVC). Inter-subject variability (third column) measured by variance ratio (VR) and coefficients of variation (CV; peak and mean activations) are also presented for MVIC (black bars) and DMVC (grey bars). Both VR and CV variability measures are unitless.

3.2. Normalization x Sex Comparisons

Results for the mixed model ANOVAs can be found in Tables 9 and 10. A significant normalization method by sex interaction was found for both peak and mean BF activation levels (p=0.005 and p=0.007, respectively), but not for peak or mean RF and VM. Post hoc tests revealed that differences between normalization methods were more pronounced in females than males for both peak (T=3.043, p=0.005, d=1.171) and mean (T=2.821, p=0.013, d=1.103) activations (Figure 10). Post hoc tests also found greater sex differences when normalizing to MVIC than DMVC for both peak (T=2.541, p=0.026, d=0.757) and mean (T=2.629, p=0.022, d=0.920) BF activations. Lastly, there were significant normalization method main effects for peak and mean activations for all muscles (all p<0.001; Tables 9 &10).

Table 9. Comparisons of peak activation levels normalized to peak MVIC and DMVC: mean±std

| | MVIC | | DMVC | | MMANOVA (F, p, η_p^2) | | |
	M	F	M	F	Interaction	Normalization	Sex
RF	2.93±1.39	2.22±1.18	0.91±0.28	0.93±0.23	2.217, 0.149, 0.081	46.163, <0.001, 0.649	1.679, 0.207, 0.063
VM*	3.47±3.08	4.69±2.94	0.69±0.20	1.09±0.39	0.049, 0.827, 0.002	98.135, <0.001, 0.797	5.474, 0.028, 0.180
BF*	0.47±0.27	1.50±1.05	0.49±0.23	0.77±0.28	9.260, 0.005, 0.270	4.772, 0.039, 0.160	18.793, <0.001, 0.429

Note: Activation data are reported as mean percentages and 1 standard deviation per normalization scheme; MVIC: maximum voluntary isometric contraction, DMVC: dynamic maximum voluntary contraction during 1-RM; RF: rectus femoris; VM: vastus medialis; BF: biceps femoris long head; M & F: male and female groups; *: Statistical test results for both VM and BF data are reported on the common logarithm transformations. MMANOVA: mixed-model ANOVA; F, p, ηp2: f-statistic, p-value, and partial eta-squared reported for interaction and main effect terms.

Table 10. Comparisons of mean activation levels normalized to peak MVIC and DMVC: mean±std

| | MVIC | | DMVC | | MMANOVA (F, p, η_p^2) | | |
	M	F	M	F	Interaction	Normalization	Sex
RF	1.37±0.53	1.29±0.61	0.43±0.11	0.55±0.12	0.779, 0.386, 0.030	56.860, <0.001, 0.695	0.024, 0.879, 0.001
VM	2.26±1.56	2.82±1.80	0.51±0.08	0.63±0.12	0.475, 0.475, 0.019	36.795, <0.001, 0.260	1.075, 0.310, 0.041
BF	0.33±0.18	0.88±0.51	0.39±0.14	0.46±0.12	8.48, 0.007, 0.253	8.762, 0.007, 0.260	17.077, <0.001, 0.406

Note: MVIC: maximum voluntary isometric contraction, DMVC: dynamic maximum voluntary contraction during 1-RM; RF: rectus femoris; VM: vastus medialis; BF: biceps femoris long head; M & F: male and female groups; MMANOVA: mixed-model ANOVA; F, p, ηp2: f-statistic, p-value, and partial eta-squared.

Figure 10. Interaction effects for peak and mean BF normalized to MVIC and DMVC

Figure 10a. Interaction effects for BF activation levels reported by logarithm transformations.
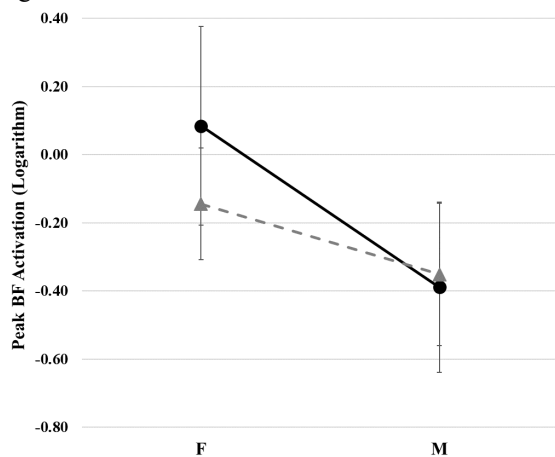
Figure 10b. Interaction effects for peak BF activation reported by activation (normalized to MVIC and DMVC).
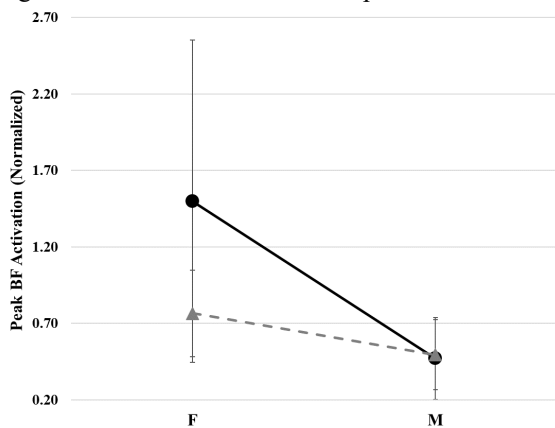
Figure 10c. Interaction effects for mean BF activation.
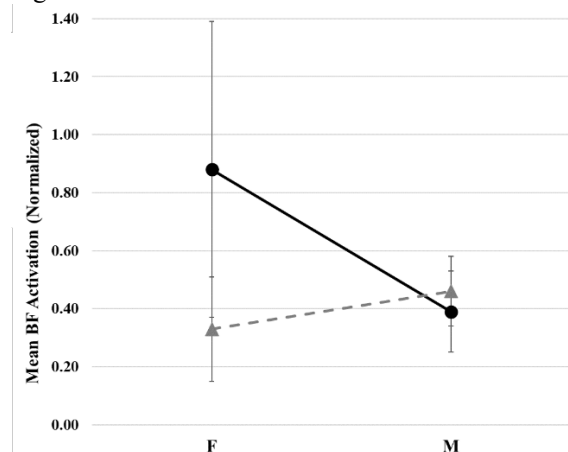
Biceps femoris (BF) peak (10a & 10b) and mean (10c) activations normalized to maximum voluntary isometric contractions (MVIC) and dynamic maximum contractions (DMVC) are represented by black lines/circles and grey lines/triangles, respectively. Standard deviations are presented as error bars. Differences between normalization schemes were larger for females than males for both peak and mean BF variables.

4. Discussion

The aim of this study was to evaluate the intra- and inter-participant variability in EMG signals, in this case males and females, when analyzed using different normalization techniques during a submaximal dynamic movement. While many EMG normalization schemes exist in the literature (A. Burden, 2010), the two chosen for this study are the most commonly used (MVIC) (Clark et al., 2012; Gene-Morales et al., 2020) and the most recommended (DMVC) (Besomi et al., 2020) given the task. The maximally weighted back squat was chosen as it is a widely used resistance exercise for both training and testing of athletes. Given the similar reliability but superior reduction in intra-group variation, the results of this study suggest the use of DMVC rather than MVIC.

4.1. Reliability

We found that normalizing to DMVC produced similar reliability for RF and BF and greater reliability for VM compared to MVIC (Table 8). In support of our findings, a review performed by Burden (2010) suggested that MVICs and submaximal contraction measurements are equally reliable (A. Burden, 2010). To date, only one previous study has evaluated reliability

of normalization methods of a lower extremity dynamic resistance exercise with an external free weight load (Balshaw and Hunter, 2012), using the free weight back squat for their analysis. Balshaw and Hunter (2012) assessed ten males and implemented a three-repetition-maximum (3RM) protocol and normalized to percentages of the 3RM task and MVIC. Normalization to the dynamic task demonstrated greater absolute reliability and sensitivity for both the vastus lateralis and BF compared to an MVIC (Balshaw & Hunter, 2012). Although implementing different tasks, Albertus-Kajee, et al. (2011) evaluated three normalization methods (MVC, sprint running, and 70% peak sprint running) of five muscles in twelve runners of undisclosed sex (Albertus-Kajee et al., 2011). The previous study found improved repeatability, intra-participant reliability, and sensitivity when normalized to sprint running compared to MVIC. Overall, the comparable/slightly improved reliability of the DMVC compared to MVIC in this study agrees with evidence from the current literature, confirming DMVC is a reliable alternative to MVIC for evaluating muscle activation during dynamic tasks.

4.2. Variability

Although a statistical comparison was not made in our study, we found dramatic improvements in VR and CV for each of the muscles analyzed (Figure 9). Specifically, VR, peak CV, and mean CV for all muscles were reduced by 24%, 48%, and 56% in DMVC compared to MVIC, respectively. Normalization to MVICs often produces values exceeding 100% of activation, indicating that the actual maneuver requires greater muscle activation than commonly present during an MVIC. Yang & Winter (1984) evaluated normalization method effects on inter-participant variability of five muscles in eleven healthy males and females. Their study found normalizing to the peak activation recorded during walking or mean of a single stride drastically reduced inter-participant variability compared to MVIC. Recently, Korak, et al.

(2020) evaluated normalization method effects on between-muscle comparisons during back squats. The previous report found MVIC produced greater variability compared to a dynamic maximum in activation differences of the RF and gluteus maximus. Similarly, Burden (2010) conducted a review of eight normalization methods and concluded that normalization to the peak or mean EMG from the task being evaluated would reduce inter-participant variability compared to MVIC or normalization to submaximal measurements (A. Burden, 2010). Several studies have shown support for DMVC normalization providing reduced inter-participant variability compared to MVIC (Allison et al., 1993; Bolgla & Uhl, 2007; A. Burden & Bartlett, 1999; A. M. Burden et al., 2003; Chapman et al., 2010; Knutson et al., 1994). Although not a fatal flaw, muscle activations normalized to MVIC achieved large supramaximal levels (Tables 8 & 9), which lends further evidence that the MVIC does not elicit a true maximum as found in the current literature. In addition, analyses of joint angles at peak activation demonstrate DMVCs are a more dynamically equivalent normalization method compared to MVICs (Table 7), which enhances relevance to the current task but can decrease generalizability to other tasks.

Given the influence of within-group variability on the stability and outcomes of statistical tests (e.g., studentized tests and ANOVAs), reduction of within-group variability should be a benefit for enhancing discrimination between groups. However, as noted previously by Yang and Winter (1984), a reduction of within-group variability is a double-edged sword as normalizing to DMVCs removes more biological variation within groups while homogenizing the data. In addition, DMVCs require special attention to methodological concerns (see Introduction) that are not necessarily involved with MVICs. Therefore, while this and the previous research support the use of DMVCs over MVICs, continuing research in this area is warranted.

4.3. Effects on Between-group Analysis

Although reducing intra-group variability and maintaining/improving reliability are of great importance, the influence of normalization on between-group analyses also deserves attention. Given that back squats are a familiar task for both sexes and that sex differences have been found in the literature (Mehls et al., 2020; Roberts et al., 2020; Youdas et al., 2007; Zeller et al., 2003), we decided to implement sex as our between-group comparison. The current study found BF activations were significantly different between sexes when normalized to MVIC but not DMVC. A possible mechanism behind the BF interaction found here are sex differences in hip extensor musculature. Females exhibit reduced hip extensor strength (Stearns et al., 2013), of which the hamstring contribute 30-48% (Waters et al., 1974), and shorter optimal BF lengths (Wan et al., 2017) compared to males. As such, it is possible females in this study depended on greater emphasis of the BF/hamstrings than males in the squat (a hip and knee dominant task), thus achieving very large BF activations relative to MVICs (the less neuromuscularly demanding task). In addition, sex differences in optimal BF muscle lengths, found at the whole muscle level using dynamometry and motion capture (Wan et al., 2017), could necessitate sex-specific postures for MVIC testing (not explored in this study). Future work is required to explore the extent to which muscle activation responses differ in posture between the sexes.

Interestingly, the RF and VM did not display significant interaction effects. The lack of significant interaction effects for RF and VM could be a product of the larger inter-subject variability found in MVIC data (Figure 9; Tables 9 & 10), which would limit the ability to identify differences. Similarly, no sex main effects were found for RF or VM, despite seemingly large differences between the sexes (Figure 11). Again, large intra-group variability for males and females in the MVIC could negatively impact the ability to detect/identify sex differences.

Although CV is sensitive to the magnitude of the data, important information can be gleaned from this metric when coupled with additional metrics (e.g., effect sizes). For example, CV of peak VM activation normalized to MVIC were 89% and 63% for males and females, respectively (Table 9), which coincided with a low Cohen's D effect size (Figure 11). However, CV for peak VM normalized to DMVC were only 29% and 36% for males and females, respectively, and coincided with an effect size greater than 1.2. Thus, in agreement with our sentiments for the BF, the DMVC appears to be the superior method for normalization with weighted exercises. In further agreement with the findings of the current study, the European group: Consensus for Experimental Design in Electromyography has denoted normalization to DMVC to be the preferred method for normalization when a true maximum is possible (Besomi et al., 2020).

Figure 11. Effect sizes for sex differences for peak and mean activation levels of all three muscles

Figure 11a. Effect sizes for sex differences for peak muscle activations normalized to MVIC and DMVC.
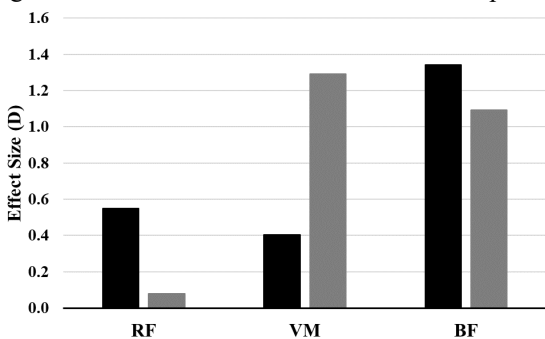
Figure 11b. Effect sizes for sex differences for mean muscle activations normalized to MVIC and DMVC.
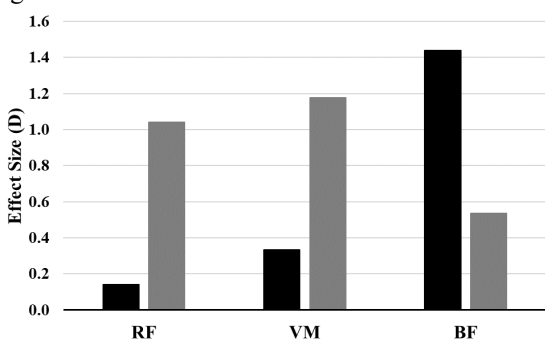
Cohen's D effect sizes for sex differences are presented for peak (11a) and mean (11b) rectus femoris (RF), vastus medialis (VM), and biceps femoris (BF) muscle activations. Black and grey bars represent activations normalized to maximum voluntary isometric contractions (MVIC) and dynamic maximum contractions (MVC), respectively.

4.4. Limitations

      There are important limitations to note with the current study. First, there are many muscles involved in the back squat that were not tested here. While others have evaluated many of the lower extremity muscles, we limited our study to three (Chuang & Acker, 2019). It is possible that these results would not exist in other muscles. Second, training level of the participants and load lifted limit the ability to compare these results to every study involving back squats. Lastly, although we followed standardized procedures, choice of filter cutoff frequency/filter order and usage of alternates to lowpass filters could influence comparisons between MVICs and DMVCs.

CHAPTER 4. INVERSE KINEMATICS DURING DEEP SQUATS: EFFECTS OF FOUR DIFFERENT FOOT TRACKING PROCEDURES

Abstract

The current literature features a dearth in methods that provide sufficient information for utilizing musculoskeletal model software to evaluate inverse kinematics (IK) in weighted full depth back squats. Thus, the purpose of this study was to directly compare different inverse kinematic strategies for calculating hip, knee, ankle, and foot kinematics utilized in modeling of the back squat. The three specific procedures explored were: 1) a weighted inverse kinematics solution, 2) utilizing a forefoot marker during dynamic trials, and 3) creating a weld constraint between the foot and the floor. The weighted back squat was chosen as it is a widely used resistance exercise. The time normalized joint angle waveforms were created separately for the eccentric and concentric phases, then recombined to ensure start, full depth, and completion of the total squat was aligned between all participants. Statistical parametric mapping and 1x4 one-way within-participants analyses of variance with alpha level set at 0.006 was used to compare the joint angles and moments between inverse kinematic evaluation conditions. The results indicated a significant main effect of model for ankle and foot kinematics. Foot kinematics displayed differences between all models and direct kinematics (DK). Significant suprathresholds were found between the control Unweighted model (larger angles) and DK in the transverse plane, the Weighted model (larger angles) and DK in all three planes, the Toe model (larger Weighted angles) and DK in the transverse and frontal planes, and the Weld model (larger angles) and DK were found in both the sagittal and frontal planes. The results indicated a significant main effect of model for hip sagittal and transverse plane and knee sagittal plane moments. The Cohen's D effect sizes for moments of the Weld model compared to the other

models were large (hip and knee sagittal plane, and hip frontal plane). The IK model whose mean foot rotations most closely matched the DK results, was the Weld model.

1. Introduction

Weighted dynamic exercises are a highly utilized tool in clinical and athletic settings. Particularly, the weighted back squat is used to evaluate everything from athletic preparedness (Myer et al., 2014) to post surgery recovery (Catelli et al., 2020). Although inverse dynamics analyses have broadened our understanding of back squats (Maddox et al., 2020; Maddox & Bennett, 2021), no aspects of the human body's response to a weighted exercise can truly be evaluated in vivo as the internal forces (e.g., muscle and joint contact) occurring during a weighted back squat cannot be measured directly. Musculoskeletal modeling is a tool for estimating forces that cannot be otherwise measured in living bodies (Hicks et al., 2015) and has been used extensively to evaluate everyday tasks such as gait, landing, throwing, and ascending/descending stairs. Musculoskeletal models combine anthropometric, marker trajectories, ground reaction force, and electromyographic (or simulated activations) data to solve for unknown muscle and joint contact forces.

Internal forces occurring during squatting maneuvers have been predicted using modeling for decades (Dahlkvist et al., 1982), albeit from a more limited perspective (e.g., single plane analyses (sagittal plane), fewer muscles and degrees of freedom). Recently, musculoskeletal models have been developed to allow for the larger hip and knee joint angles required for squatting movements (D. S. Catelli et al., 2019; Lai et al., 2017). These studies have evaluated kinematics (Li et al., 2021) joint moments (Bini et al., 2021; Li et al., 2021; Wolf et al., 2021), muscle forces (Bini et al., 2021; Golfeshan, Barnamehei, Torabigoudarzi, et al., 2020; Kipp et al., 2022b; Wolf et al., 2021), and joint contact forces (Bedo et al., 2020; Bini et al., 2021; Catelli

et al., 2020; Song et al., 2022). So far, the previous studies primarily focused on the hip and knee with little to no attention paid to the ankle. The focus on hip/knee joints is expected as a majority of the joint moments during a weighted back squat are going to occur at the hip (~50%) and knee (~30%) as their distance from the center of mass increases (Maddox & Bennett, 2021). Although the ankle moment is quite small in comparison (~20%), the ankles are very important for proper movement mechanics in both sport and weightlifting (Demers et al., 2018; Fuglsang et al., 2017; Gomes et al., 2020; Maddox & Bennett, 2021).

Several studies have evaluated ankle characteristics during squats using OpenSim models (Bini et al., 2021; Bordron et al., 2021; Golfeshan, Barnamehei, Torabigoudarzi, et al., 2020; Li et al., 2021; Wolf et al., 2021). Bini et al. (2021) reported mean (of 5 repetitions) sagittal plane moments of the ankle for eleven male participants performing weighted front and back squats. While no significant differences were seen in ankle moments between conditions, large standard deviations within each condition allude to high inter-participant variability of ankle moments (Bini et al., 2021). Li et al. (2021) evaluated range of motion and moments for hips, knees, and ankles of sixteen female participants performing bodyweight full depth and half squats. The study reported larger ankle plantarflexion moments during the half squat than the full depth squat (Li et al., 2021). Wolf et al. (2021) investigated net moments and relative muscular effort (net moment vs. "maximum possible moment"; maximum possible moment was defined by summing all maximally active positive extensor muscle moments at each joint) for each lower extremity joint in nine male participants performing a weighted back squat. The study reported no significant difference in ankle relative muscular effort between loads (maximum load lifted was 38% of the participants back squat one-repetition-maximum (1RM)) (Wolf et al., 2021). Golfeshan et al. (2020) reported significant differences (magnitude not reported) in medial

gastrocnemius forces between two conditions evaluated (hands behind the head and hands in front of the chest) while performing bodyweight squats. Despite the information that can be gleaned from the previous research (Li et al., 2021; Wolf et al., 2021), the lack of specification on their modeling procedures (e.g., inverse kinematic parameters, etc.) makes replication or implementation of the methods very difficult.

The foot is the first point of contact in a squat and any inaccuracies could have important impacts on the resultant calculations. Ankle moments are highly dependent on the accuracy of the joint kinematics (Riemer & Hsiao-Wecksler, 2008). When collecting experimental 3D motion capture data of full depth squats, any unexpected displacement of the foot will likely be attributed to model defined constraints based on tibial movement such as adduction and internal rotation or limitations of the model to reach full depth (e.g., exceeding maximum hip flexion of 120°). When using a model designed for full depth squats to evaluate a participant moving through the entire squat maneuver, two issues are present: 1) the feet are shown to translate and rotate, whereas the feet did not move during experimental data collections and 2) the ankle joint angles are quite different from direct kinematic models (Figure 1). This suggests that either previous studies also had issues with the feet and did not acknowledge the limitation in their manuscript or did not have issues through modifying standard procedures (e.g., changing weight schemes for inverse kinematics) which were not specified.

While some information toward preferred methods of conducting inverse kinematics in OpenSim have been alluded to in the literature (Bedo et al., 2020; Bini et al., 2021; Bordron et al., 2021; Catelli et al., 2019; Golfeshan, Barnamehei, Torabigoudarzi, et al., 2020; Kipp et al., 2022a; Li et al., 2021; Y. Lu et al., 2020; Z. Lu et al., 2022; Sinclair et al., 2022; Song et al., 2022; Wolf et al., 2021)., the majority did not describe their methods with enough detail to

replicate. For instance, some studies mention the number of markers used with locations either not mentioned or ambiguously described (e.g. " distinct anatomical landmarks") (Bedo et al., 2020; Bordron et al., 2021; Goodman, 2020; Song et al., 2022). Or, instead of describing which markers were used, a citation was made to a study that does not identify the specific markers used (Bedo et al., 2020; Catelli et al., 2019; Li et al., 2021; Y. Lu et al., 2020). While some make no mention of markers at all (Bini et al., 2021; Lu et al., 2022). There were a couple of researchers that meticulously described marker locations (Kipp et al., 2022a, 2022b; Sinclair et al., 2022; Wolf et al., 2021) or at least provided a reference for a specific marker set used (Catelli et al., 2020). While it is likely all the previous literature implemented traditional IK models (non-weld), which may produce similar kinematic waveforms for proximal joints, none of these methods (which were most likely included in the current literature) are sufficient for tracking foot kinematics. Regardless of method, it is imperative the current literature base improves its reporting.

The purpose of this study was to directly compare different inverse kinematic strategies utilized in modeling of the back squat. Four specific procedures stand out as the most applicable to be evaluated in back squats. First, a weighted inverse kinematics solution that normalizes the weighting scheme by the size (resultant vector) of the marker system for each segment. The larger the weight of the marker system for a segment, the more closely the least-squares equation will match the location of the markers than those weighted lower. The foot segment is dramatically smaller than the other segments of the lower extremity. Applying a larger weight for the foot segment should improve tracking/matching. A recent study used segment lengths to normalize the weighting scheme for their inverse kinematics analysis (Bordron et al., 2021). The study evaluated the estimated joint moments using an OpenSim model compared to the

calculated joint moments using a MATLAB model, and no kinematic data was reported. Second, as plantarflexion of the foot during the descent phase of a back squat was not observed during experimental data collection in any participant, altering the model to include a weld joint between the feet and the floor needs to be explored. The previous study that weighted the least squares equation for inverse kinematics using segment lengths, also created a weld joint between the foot and the floor, indicating they too may have observed issues with plantarflexion of the model during the squat (Bordron et al., 2021). Third, the standard experimental marker set used for data collections typically does not include forefoot (e.g., toe, metatarsal heads, etc.) marker during dynamic trials (Braidot et al., 2007; M. Bryanton et al., 2012; Diggin et al., 2011; Escamilla, Fleisig, Zheng, et al., 2001; Lynn & Noffal, 2012; Mackala et al., 2013; Miletello et al., 2009; Niu et al., 2010; Stearns et al., 2013). However, a marker located at the toe would assumedly provide enough information regarding the foot orientation to constrain the inverse kinematics model to fit experimental foot kinematics. Finally, an unweighted model will serve as a control comparison. We hypothesize the foot-floor weld procedure, and the toe marker procedure will produce the most accurate inverse kinematic results compared to experimentally collected data, as they will constrain the model to the position of the participant during the weighted back squat. Furthermore, we hypothesize the joint moments produced from the foot-floor weld and toe marker procedures will closely match, but display differences compared to the Unweighted control and Weighted procedures.

2. Methods

2.1. Participants

This study was approved by the Old Dominion University Institutional Review Board. A subset of nine resistance-trained individuals with no history of knee injuries, age 18-55 years,

who perform weighted squats at least 1 day per week for at least one-year at or near maximal loads that participated in previous studies (Maddox et al., 2020; Maddox & Bennett, 2021) were utilized in this study. Participants were excluded if they had any lower extremity injuries in the past 3 months, knee pain in the past 6 months, a diagnosis of lower extremity joint arthritis, or a body mass index (BMI) greater than 35 kg·m^{-2}. All participants were informed of the study procedures and signed consent forms as previously described (Maddox et al., 2020; Maddox & Bennett, 2021).

2.2. Procedures

A ten-camera motion capture system (200Hz, Vicon Motion Analysis Inc., Oxford, UK) was used to collect 3D marker coordinates. Reflective markers were placed bilaterally on anatomical landmarks: iliac crests, anterior superior iliac spines, posterior superior iliac spines, greater trochanters, femoral epicondyles, medial and lateral tibal condyles, medial and lateral malleoli, first and fith metatarsal heads, and second toes as previously described (Maddox et al., 2020; Maddox & Bennett, 2021). Additionally, 4-marker clusters were placed bilaterally on the posterior mid trunk, posterior pelvis, lateral mid shank, lateral mid thigh, and lateral posterior shoe. The anatomical landmark markers (excluding toe) were removed after the static trial, and the 4-marker clusters remained in place for the dynamic trials, as is standard in our lab (Weinhandl et al., 2010, 2021). A traditional style barbell rack, barbell (20.5 kg) and weighted plates were placed around the center of the motion capture collection area and two force platforms (2000Hz, Bertec FP-4060, Bertec Inc. OH, USA). Force platforms collected ground reaction forces (GRFs) applied to each foot segments during the entirety of each repetition.

Prior to beginning the 1RM (one-repetition-maximum) testing, participants were allowed five minutes for warming up and stretching of their choice. Next, participants completed the

NSCA's 1RM testing protocol (Haff & Triplett, 2016) as described in detail in our previous work (Maddox & Bennett, 2021).

2.3. Musculoskeletal Modelling

This study used previously recorded marker trajectories collected as described (Maddox et al., 2020; Maddox & Bennett, 2021) to generate participant-specific models (i.e., anthropometric scaling) using OpenSim (v4.1, SimTK, Stanford, CA) and the Catelli 2019 model (Catelli et al., 2019). The Catelli 2019 model is an update to the popular Lai 2017 model (Lai et al., 2017), specifically derived to allow deeper hip and knee flexion. Both models consist of 37 degree-of-freedom (dof): 20 for the lower body (6-dof for the pelvis, and 7-dof per leg), 17 for the torso (3-dof for the lumbar joint) and upper body (7-dof per arm), 80 lower extremity Hill-type muscle-tendon units (40 per leg) with 40 wrapping surfaces, and 17 torque actuators for the torso/arms. However, the Catelli 2019 model was created to specifically accommodate deep squat maneuvers: 1) increased the model's knee flexion capabilities from 140° to 145°, 2) increased the model's hip flexion capabilities from 120° to 138°, and 3) added wrapping surfaces of muscles about the knee joint. The alterations allow for the large hip and knee motions required to achieve a deep squat and improve muscular functions for the deep range of motions.

Scaling and marker registration of the generic Catelli 2019 models were performed using participant mass, segment lengths, pose, and marker start locations from direct kinematic models derived in Visual3D (Maddox et al., 2020, 2022; Maddox & Bennett, 2021). Foot markers were assigned to the calcaneus and toe markers were assigned to the toes (when included). The subtalar joint was unlocked for all models as the subtalar joint is required in the weld model (toes welded to ground). Given no other dofs, the foot was considered a single body from calcaneus to toes. Inverse kinematics and inverse dynamics were used to derive body and joint movement

patterns and net internal moments from the participants' experimental marker trajectories in four different ways: 1) a control procedure using an equal weighted (for each segment) least-squares inverse kinematics evaluation (Unweighted model) (Spoor & Veldpaus, 1980), 2) a custom weighted least-squares approach (Spoor & Veldpaus, 1980) using the length of the segment (average pelvis width = 0.23m, thigh length = 0.41m, shank length = 0.40m, trunk length = 0.40m, foot length = 0.14m; Weighted model) (Bordron et al., 2021), 3) altering the Unweighted model to include a weld constraint between the toes and the ground (Weld model; adapted from Bodies+WeldConstraint.osim by Ajay Seth), and 4) foot tracking cluster and the toe marker unweighted (Toe model). The first three listed models only used the tracking cluster located on the posterolateral heel.

Preliminary analyses proved weighting by segment length did not improve foot marker tracking nor did it change any kinematics from the Unweighted model. Following this, we systematically increased the weight of the foot markers by 100% until notable changes (i.e., improvement) in foot kinematics was achieved. Weighting of foot tracking required a 10-times relatively greater emphasis on foot markers. Subsequent analyses and reports include this weighting scheme for the Weighted model.

2.4. Data Analysis

The joint angle and moment waveforms derived using OpenSim were imported into MATLAB (R2021b). Time normalized waveforms were created separately for the concentric (upward) phase (51 time points) and eccentric (downward) phase (50 time points) and then recombined to ensure start, full depth, and completion of the total squat was aligned between all participants. The eccentric phase was defined as the time between the initial downward motion of the model center of mass (downward velocity >0.01 m/s) and when the body reached full

depth (maximum knee flexion). The concentric phase was defined as the time between the body reaching full depth to standing upright (upward velocity <0.01 m/s).

Mean and standard deviation (SD) waveforms were created for each model for all eight variables: hip (sagittal, frontal, and transverse planes), knee (sagittal plane), ankle (sagittal plane), and foot (sagittal, frontal, and transverse planes) angles (Figure 12) and moments (Figure 13).

Figure 12. Ensemble mean and SD of hip, knee, ankle, and foot rotations.
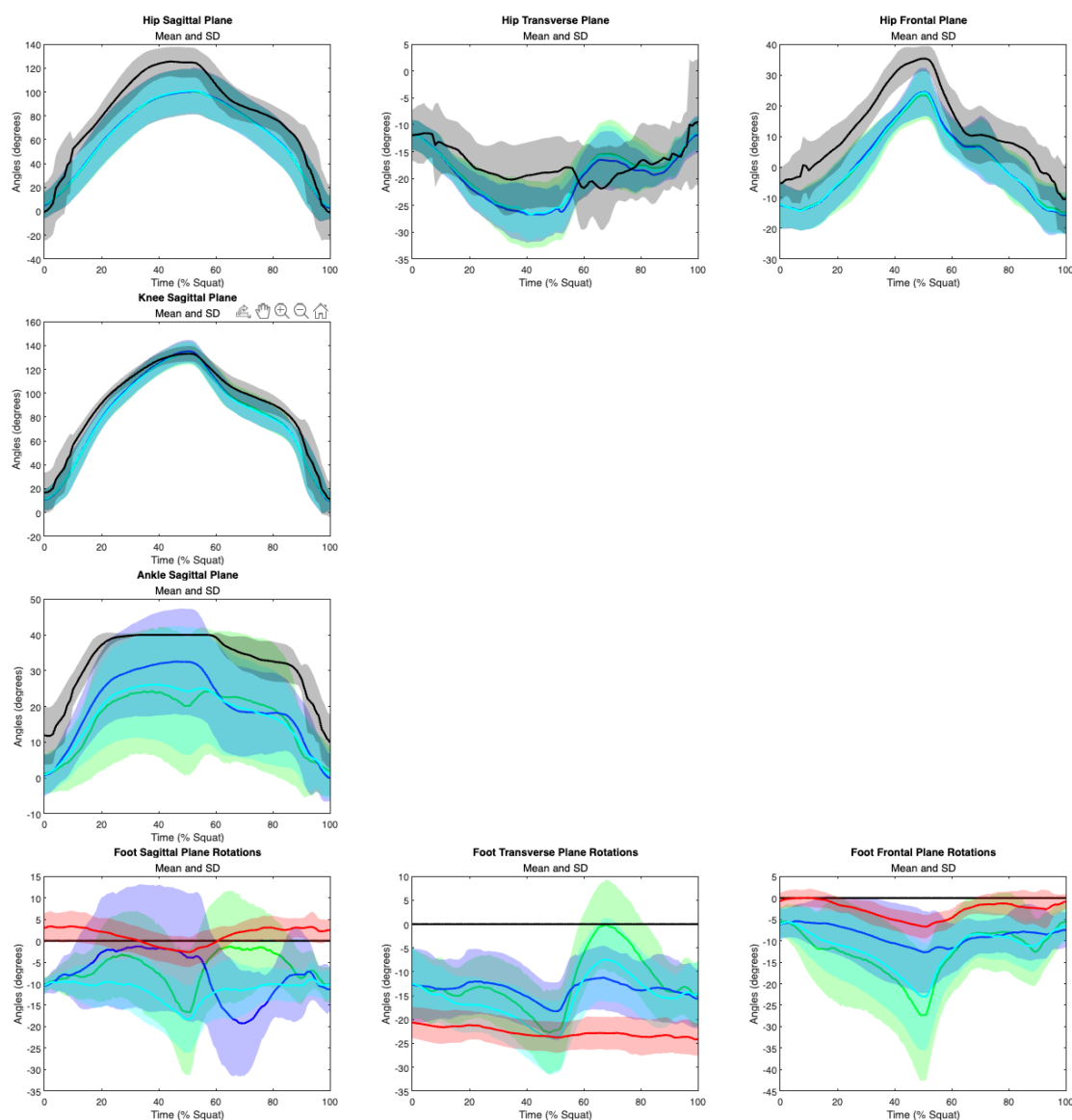
Means and one standard deviation are presented for Unweighted model (green), Toe marker model (blue), Weighted model (cyan), Weld model (black), and Direct kinematics (DK) (red). Positive angles indicate dorsiflexion (ankle

and foot), foot internal rotation, and foot adduction. Negative angles indicate plantarflexion (ankle and foot), foot external rotation, and foot abduction.

Figure 13. Ensemble mean and SD of hip, knee, and ankle moments.
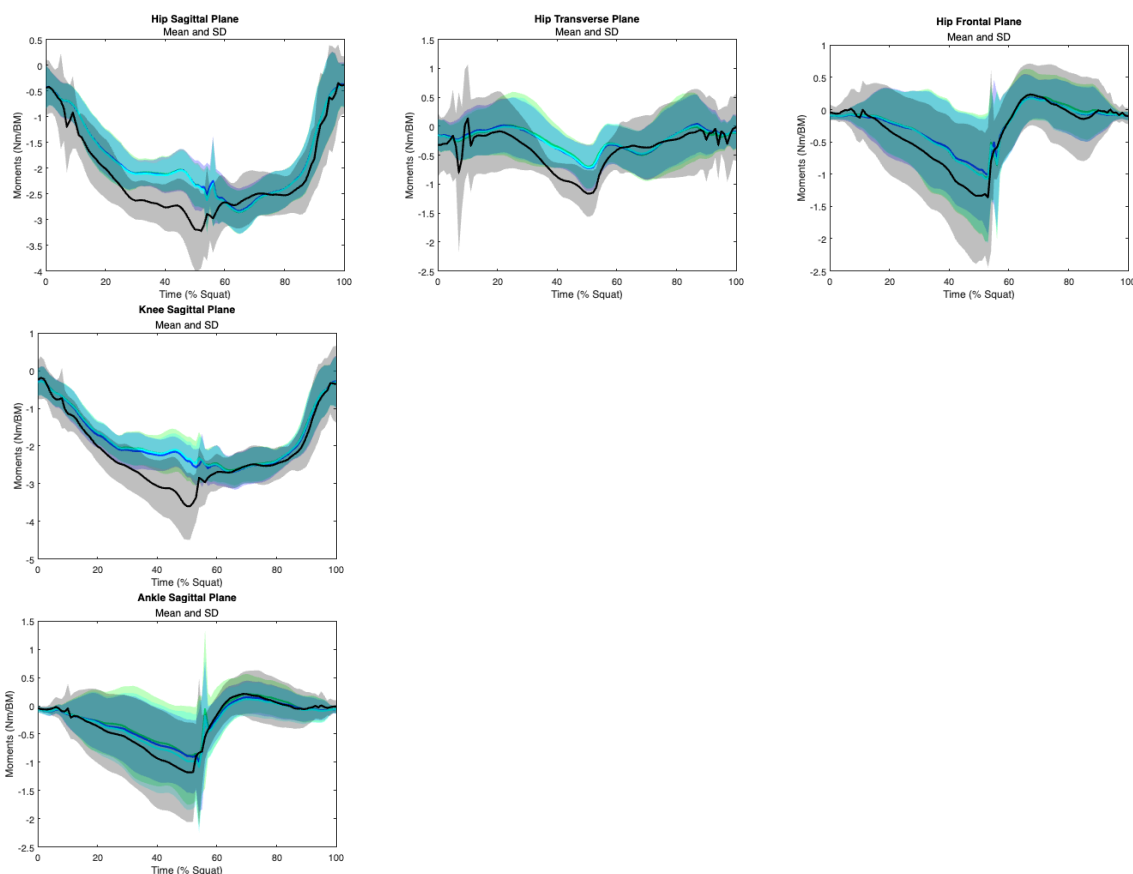
Means and one standard deviation are presented for Unweighted model (green), Toe marker model (blue), Weighted model (cyan), and Weld model (black). Positive moments indicate flexion (hip and knee), hip internal rotation, hip adduction, and ankle dorsiflexion.

2.5 Statistical Analysis

Statistical parametric mapping (SPM{f}) one-way (4-inverse kinematic models) within-participants analyses of variance (ANOVAs) with alpha level set at 0.006 (constrained based on number of variables, i.e., alpha at <0.006, reduced from 0.05 to limit type I errors) were used to compare the hip (tri-planar), knee (sagittal plane), and ankle (sagittal plane) joint angles and moments between inverse kinematic evaluation conditions (Unweighted, Toe, Weighted, and Weld) (spm1d.org; v.M0.4; (Pataky et al., 2008)). The statistical parametric map was created using the scalar output statistic, SPM{f}, for each time point. To test the null hypothesis, a

critical threshold SPM{f} was computed such that only 0.6% of smooth random curves would exceed the threshold. Prior to performing comparisons, normality of each variable was assessed using the open-source software. When normality concerns were present, non-parametric tests were performed. Supra-threshold clusters were identified as multiple adjacent points of the SPM{f} curve exceeding the 0.6% threshold. Suprathreshold clusters with a width of less than five were considered not meaningful and are not reported here. Post hoc dependent SPM{t}tests (alpha level 0.006) were performed in the presence of a statistically significant ANOVAs. Timing of suprathreshold clusters, mean differences, F-statistic, and p-values were extracted from the SPM{f} ANOVAs and post hoc SPM{t} tests. Effect sizes (Cohen's D) were also derived and presented for statistically significant model comparisons (small: 0.2-0.49 , moderate: 0.5-0.79, and large: >0.8) (Cohen, 1988).

One-way within-participants SPM{f} ANOVAs with alpha level set at 0.006 were used to compare the foot rotations amongst Unweighted, Toe, and Weighted inverse kinematics and DK. Considering the foot cannot move in the weld constraint model, we separately compared the Weld model and DK using dependent SPM{t} tests (alpha at <0.006) instead of including the Weld in the ANOVAs for the foot, which avoids the large and unnecessary influence this model would have on the ANOVAs.

3. Results

ANOVA statistical parametric maps with supra-threshold clusters, and their corresponding p-values are presented in Tables 11 & 12. Post-hoc results, including mean difference between conditions during the reported statistically significant time range, achieved p-values and the mean difference between conditions during the reported statistically significant time range, are presented below (Table 13).

Table 11. Joint kinematic ANOVA test results.

Variable	ANOVA (F, loc, p)
Hip Flexion/Extension	9.0, 9-59 & 77-91, <0.001
Hip Int/External Rotation	Not Significant
Hip Add/Abduction	9.5, 5-61 & 75-97, <0.001
Knee Flexion/Extension	9.6, 7-29 & 60-92, <0.001
Ankle Dorsi/Plantarflexion	9.1, 0-20 & 59-100, <0.001
Foot Sagittal Plane	9.3, 0-11 & 67-79 & 95-100, <0.003
Foot Transverse Plane	7.3, 0-100, <0.001
Foot Frontal Plane	6.7, 0-36 & 56-100, <0.001

F, loc, and p: F-statistic, location (percent of squat), and p-value threshold exceeded.

Table 12. Joint moment ANOVA test results.

Variable	ANOVA (F, loc, p)
Hip Flexion/Extension	9.0, 10-19, 21-53 & 88-90, <0.001
Hip Int/External Rotation	9.3, 24-31 & 33-58, <0.001
Hip Add/Abduction	Not Significant
Knee Flexion/Extension	9.5, 32-53, <0.001
Ankle Dorsi/Plantarflexion	Not Significant

F, loc, and p: F-statistic, location (percent of squat), and p-value threshold exceeded.

3.1. Ankle and Foot

The SPM{f} ANOVA results indicated a significant main effect of model for ankle and foot kinematics (Table 11). The SPM{f} ANOVA results indicated no main effect of model for ankle moments (Table 12).

Suprathreshold clusters in post hoc tests SPM{t} of kinematics were found at the ankle and foot (Table 13). A significant suprathreshold was found for the Weld model compared to the Unweighted model, the Toe model, and the Weighted model (Table 13). Suprathreshold clusters in post hoc tests were found for foot orientations between all models and DKs. Significant suprathreshold clusters in post hoc tests were found between the Unweighted model (larger

angles) and DK in all three planes. Significant suprathreshold clusters in post hoc tests were found between the Weighted model (larger angles) and DK in the sagittal and frontal planes. Significant suprathreshold clusters in post hoc tests were found between the Toe model (larger angles) and DK in the frontal plane. Significant suprathreshold clusters in post hoc tests were found between the Weld model (larger angles) and DK in the frontal plane (Table 13). Interestingly, the differences found between the Weld model and DK spanned less than 12% of the squat in the frontal plane.

3.2. Hip and Knee

The SPM{f} ANOVA results indicated a significant main effect of model for hip sagittal and transverse plane and knee sagittal plane kinematics (Table 11). The SPM{f} ANOVA results indicated a significant main effect of model for hip sagittal and transverse plane and knee sagittal plane moments (Table 12).

In performing post hoc tests SPM{t} of hip and knee kinematics, we found no significance. The reason for the disagreement between the SPM{f} ANOVA results and the post hoc SPM{t} tests is due to the lack of variability between the three non-weld models (see Figures 12-13) and the fact that ANOVAs incorporate variability across all conditions while post hoc SPM{t} tests do not. While post hoc methods such as Tukey's Honest Difference tests incorporate variability across multiple groupings, these tests are not currently available in SPM. In contrast to reporting post hoc SPM{t} tests, we decided to provide effect sizes (Cohen's D) between the Weld model and the other three models. The effect sizes for the hip in the sagittal plane for the Weld compared to Unweighted model (0.98), Toe model (0.95), and Weighted model (0.96) were large. The effect sizes for the hip in the frontal plane for the Weld compared to Unweighted model (1.38), Toe model (1.38), and Weighted model (1.41) were large. The

effect sizes for the knee in the sagittal plane for the Weld compared to Unweighted model (0.88),

Toe model (0.87), and Weighted model (0.96) were large.

Table 13. Joint kinematic post-hoc test results.

Variable	Unweight-Weld (Diff, loc, p)	Unweighted-DK (Diff, loc, p)	Toe-Weld (Diff, loc, p)	Toe-DK (Diff, loc, p)	Weight-Weld (Diff, loc, p)	Weight-DK (Diff, loc, p)	Weld-DK (Diff, loc, p)
Ankle	-18.92±11.98, 9-15, 0.002; -19.67±11.88, 88-92, 0.002; -17.18±10.53, 92-95, 0.002	N/A	-13.64±8.75, 10-11, 0.002; -15.21±8.90, 67-96, 0.002	N/A	-16.37±9.66, 9-15, 0.002; -17.16±9.37, 82-95, 0.002	N/A	N/A
Foot Sagittal	N/A	-12.64±4.54, 0-7, 0.001	N/A	Not Significant	N/A	-9.55±3.27, 0-11, 0.001; -12.86±5.66, 79-100, 0.001	Not Significant
Foot Transverse	N/A	20.55±8.55, 61-79, 0.002	N/A	Not Significant	N/A	Not Significant	N/A
Foot Frontal	N/A	-17.60±12.21, 41-54, 0.002	N/A	-7.44±5.51, 64-80, 0.002	N/A	-8.32±6.59, 7-18, 0.002; 913.61±9.97, 36-55, 0.002; -8.60±6.54, 85-92, 0.002	5.97±2.57, 48-60, 0.002

Diff, loc, and p: mean difference ± 1 standard deviation, location (percent of squat), and p-value threshold exceeded.

4. Discussion

The aim of this study was to compare kinematics and moments between four inverse kinematic procedures. Furthermore, foot segment kinematics were compared with standard DK results of a weighted back squat. The Weld model's foot rotations most closely matched the DK results for the sagittal and frontal planes. However, the transverse plane rotations were offset ~20 degrees between the Weld model because the calcaneus cannot be rotated. While the Weld model presented with the foot rotations that matched closest with DK results, this model presented with significantly increased proximal (hip, knee, ankle) joint rotations and (hip, knee) moments compared to the other models. In contrast, this study found mean hip, knee, and ankle

kinematics and moments were not different between traditional IK models (Unweighted, Toe, and Weighted models). As the impact of foot modeling certainly does not stop at kinematics and inverse dynamics (e.g., downstream analyses such as muscle force predictions as all the shank muscles attach below the subtalar joint), authors must exercise caution and be more transparent regarding their modeling procedures.

The moment differences found in the hip and knee are likely due to the orientation of the hip joint created by the forced parallel configuration of the feet when a weld constraint is included. Although we expected to find significant ankle moment model effects given the differences found in ankle/foot kinematics, the relationship between moments and joint angles is not straight forward. The lack of differences in ankle joint moments, despite the large differences in ankle and foot kinematics (Table 13), is likely a result of the model degree-of-freedom constraints' effects on global positioning. For instance, the location of the foot (like an end effector) is impacted by the translations and orientations of the proximal segments/joints, of which the pelvis and hip typically contain the greatest dof. Thus, the differences we found between the weld and non-weld models in all three planes of hip kinematics could have altered ankle joint locations relative to the ground reaction force.

A majority of squat studies focus on the hip and knee joints as they account for a majority of the load distribution during back squats (~50% at the hip and ~30% at the knee) (Flanagan et al., 2003, 2015; Flanagan & Salem, 2008; Fry et al., 2003; Gullett et al., 2009; Hirata & Duarte, 2007; Jaberzadeh et al., 2016; Kubo et al., 2018; Lorenzetti et al., 2012; Maddox & Bennett, 2021; Schoenfeld, 2010; Yavuz et al., 2015). The Toe, Weighted, and Unweighted model's moment waveforms are almost identical, with the Weld model showing larger moments leading up to and at maximum depth. Our current results were similar in the sagittal plane for the hip,

larger for the knee, and smaller for the ankle moments than previously reported using bottom-up

inverse dynamics and a 6-dof model of maximal weighted back squats (Maddox & Bennett,

2021). Furthermore, the moments produced by all the models at all joints were comparable to

other squat modeling studies that utilized the same model with unweighted full depth squats (Li

et al., 2021; Lu et al., 2020). In contrast, one study which utilized the same model found

substantially smaller moments in the sagittal plane hip, knee and ankle. However, it is important

to note the previous study implemented squats in a smith machine and did not exceed 90° of

knee flexion (Bini et al., 2021). The only other similar study did not report any results regarding

their investigation into moments (Wolf et al., 2021).

Unfortunately, elucidating how researchers approached weighting (or not weighting) their

least-squares equation for inverse kinematics turned out to be a challenge as well. As evidenced

by the initial decision to utilize segment lengths for weighting the least-squares equation and

needing to course correct and perform the 10-times weighting of the foot markers presented in

the results. Incremental increases in weighting were attempted with little effect. Interestingly,

weighting the foot markers 10-times more heavily did not result in a significant difference in

hip/knee kinematics from the other traditional models (Figure 18) or from other published hip

and knee kinematics (Heredia et al., 2021; Li et al., 2021; Maddox & Bennett, 2021; Zawadka et

al., 2020). When the literature was explored to elucidate the weighting scheme of choice, several

studies made no mention of any adjustments (or lack thereof) to the least-squares kinematic

equation (Bedo et al., 2020; Bini et al., 2021; Golfeshan, Barnamehei, Torabigoudarzi, et al.,

2020; Kipp et al., 2022b; Sinclair et al., 2022; Song et al., 2022). Or it was simply stated that

marker weights were manually adjusted with no further details (Lu et al., 2022). One study used

CT to identify marker placement for ASISs, PSIS, and medial and lateral knees so those markers

were weighted 10-times higher (Catelli et al., 2020). And another one used segment lengths to weight the least-squares equation (Bordron et al., 2021), with no details about how they used the segment lengths to adjust their equation. Again, the lack of homogeneity in the literature regarding IK weighting methods is unsurprising considering our study found significant differences between the Weighted model and DK results for foot rotations in all three planes. Furthermore, only one squat modeling group addressed possible marker error by providing a root mean squared error threshold as the maximum acceptable error <0.04 meters (Lu et al., 2020; Lu et al., 2022). While two other research groups mentioned calculating marker errors (Kipp et al., 2022a; Kipp & Kim, 2021; Li et al., 2021; Wolf et al., 2021), no other reporting of marker errors was found in the squat modelling literature (Bedo et al., 2020; Bini et al., 2021; Bordron et al., 2021; Catelli et al., 2019; Catelli et al., 2020; Golfeshan et al., 2020; Song et al., 2022).

Figure 14. Hip and knee angles of a single subject with segment length and 10 x greater weighting on the foot.
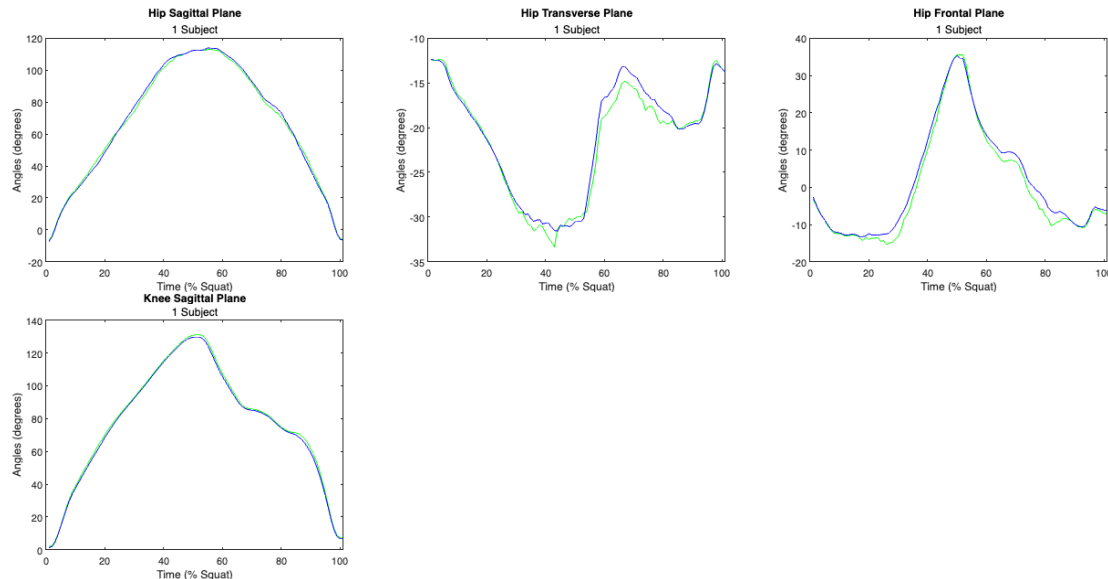
Angles are presented for segment length weighted model (green) and weighted model (blue).

Most squat evaluations focus on the hip and knee, because these joints have large ranges-of-motion and loads (Maddox & Bennett, 2021). However, the ankle and foot are important variables when using musculoskeletal modeling to predict muscle forces (Sinclair et al., 2022).

In this study, we show that choice in IK model significantly affects the rotations of the foot and ankle, the primary points of contact with the ground reaction forces. As such, the significant differences found in lower extremity kinematics and joint moments could impact muscle force predictions, which are a product of inverse dynamics and muscle state variables (e.g., moment arm, length, contraction velocity). Thus, muscle force predictions reported in the literature, which are often used as the focal points for training programs or to evaluate post-operative changes (Catelli et al., 2020), should be further evaluated based on the findings of the current study. Sinclair et al. reported significant differences in muscle forces predicted when evaluating back squats with different foot placement angles (Sinclair et al., 2022). Additionally, Lu et al. found that participants with rearfoot valgus compared with normal foot start rotations result in differences in sagittal and frontal plane hip and knee kinematics and sagittal plane ankle kinematics during back squats (Lu et al., 2022). This is not surprising considering traditional IK models do not track foot kinematics well. Despite the foot being the only contact with the ground, attention is rarely paid to foot kinematics in the literature. Although no significant differences in ankle moments were found, ankle moments have been shown to be highly dependent on the accuracy of the results of inverse kinematics (Riemer & Hsiao-Wecksler, 2008). As using different marker sets can cause comparisons between studies to be unreliable (Coyne et al., 2021), resultant kinematics from different inverse kinematics procedures could result in different down-stream estimations such as muscle forces (Mantovani & Lamontagne, 2017). Schellenberg et al. reported large overestimations of joint contact forces compared to instrumented knees when greater than 80-degrees of knee flexion was reached (Schellenberg et al., 2018). Thus, accurately calculating inverse kinematics is of great importance if the goal is to predict muscle kinetics.

While the Weld model appears to provide the best agreement with DK foot results, the IKs from the Weld model produced larger hip sagittal and frontal plane angles and substantially higher (~10°) sagittal plane ankle angles than the other models. Interestingly, the sagittal knee IKs closely match those of the other models. However, the ankle dorsiflexion angles max out the model (40°) for ~30% of the of the squat (surrounding full depth). The Weld model ankle results are likely incorrect, as maximum ankle dorsiflexion in the back squat has been found to be ~30° (Hemmerich et al., 2006). The resultant Weld model ankle kinematics are likely a result from completely constraining the motion of the foot and the joint constraints typical of inverse kinematics and specific to the model used in this study (e.g., 1-dof knee motion).

The results of this study should be considered with respect to its limitations. First, the incremental increases in weighting for the Weighted model were attempted with little effect. This result is likely due to the proximity of the foot cluster markers to each other. Future research could examine the influence of markersets positioned in multiple areas across the foot. However, given the lack of influence of a toe marker, it is possible the findings of this study are generalizable to multiple foot marker sets. Second, as IK models were the focus of this study, resultant joint and muscle kinetics were not extensively explored. The effects of each IK model on resultant joint and muscle kinetics would increase the argument for use of each IK model. Lastly, the IK models in OpenSim have spline functions to account for frontal and transverse plane rotations and translations of the knee, and fewer available degrees-of-freedom at the ankle than DK, making expectations of absolute agreement between OpenSim IKs and Visual3D DKs unlikely. However, reliability between DK and IK models has been presented (Horsak et al., 2018), with observed differences between methods being found as continuous offsets in results similar to those seen in this study.

In conclusion, we provide evidence of the effects of IK and foot modeling procedures on lower extremity kinematics and dynamics during the weighted full depth back squat. Creating a weld constraint to restrict the model to the movement of the feet found using DK allows for appropriate sagittal and frontal plane foot kinematic results. However, caution should be used when implementing weld constraints on the foot as the ankle range of motion appears untenable. In addition, the Weld model produced substantially different hip and knee moments compared to the non-weld models. However, all models produced comparable hip and knee kinematics and moments to other studies that evaluated full depth back squats. Regardless of chosen method, authors should be more transparent and forthcoming regarding their modeling procedures.

CHAPTER 5. CONCLUSION

This dissertation aimed to increase our understanding of the weighted back squat. We evaluated the different methodological processes for assessing different components of the back squat found in the literature. First, we identified three important factors for successful maximal back squats: 1) vertical acceleration is a greater discriminatory measure than velocity for analyzing successful/unsuccessful maximal back squats, 2) submaximum squats performed at increased velocities can elicit similar ankle and knee contributions as maximal squats, but the same is not true at the hip, and 3) hip strength throughout the range of motion of a squat need to be emphasized. Second, we provided evidence for the use of the peak muscle activation measured during a 1RM test as the most appropriate normalizing variable for submaximal tests of weighted back squats. Finally, we provide a solution for evaluating IKs in weighted full depth back squats. While utilizing a weld constraint to restrict the foot movement of the model results in the most DK comparable foot kinematics, restricting all foot movement with the weld constraint results in untenable ankle IKs and significantly increased sagittal plane hip, knee, and ankle moments that could affect further analysis.

REFERENCES

Abelbeck, K. G. (2002). Biomechanical model and evaluation of a linear motion squat type exercise. *Journal of Strength and Conditioning Research*, *16*(4), 516–524. https://doi.org/10.1519/00124278-200211000-00005

Akhundov, R., Saxby, D. J., Diamond, L. E., Edwards, S., Clausen, P., Dooley, K., Blyton, S., & Snodgrass, S. J. (2022). Is subject-specific musculoskeletal modelling worth the extra effort or is generic modelling worth the shortcut? *PLoS ONE*, *17*(1 1), 1–16. https://doi.org/10.1371/journal.pone.0262936

Albertus-Kajee, Y., Tucker, R., Derman, W., Lamberts, R. P., & Lambert, M. I. (2011). Alternative methods of normalising EMG during running. *Journal of Electromyography and Kinesiology*, *21*(4), 579–586. https://doi.org/10.1016/j.jelekin.2011.03.009

Allison, G. T., Marshall, R. N., & Singer, K. P. (1993). EMG signal amplitude normalization technique in stretch-shortening cycle movements. *Journal of Electromyography and Kinesiology*, *3*(4), 236–244.

Anderson, F. C., & Pandy, M. G. (2003). Individual muscle contributions to support in normal walking. *Gait and Posture*, *17*(2), 159–169. https://doi.org/10.1016/S0966-6362(02)00073-5

Arandjelović, O. (2010). A mathematical model of neuromuscular adaptation to resistance training and its application in a computer simulation of accommodating loads. *European Journal of Applied Physiology*, *110*(3), 523–538. https://doi.org/10.1007/s00421-010-1526-3

Arnold, A. S., Salinas, S., Hakawa, D. J., & Delp, S. L. (2000). Accuracy of Muscle Moment Arms Estimated from MRI-Based Musculoskeletal Models of the Lower Extremity.

Computer Aided Surgery, *5*(2), 108–119. https://doi.org/10.3109/10929080009148877

Balshaw, T. G., & Hunter, A. M. (2012). Evaluation of electromyography normalisation methods for the back squat. *Journal of Electromyography and Kinesiology*, *22*(2), 308–319. https://doi.org/10.1016/j.jelekin.2011.11.009

Barbero, M., Merletti, R., & Rainoldi, A. (2012). Atlas of muscle innervation zones. In *Atlas of Muscle Innervation Zones*. https://doi.org/10.1007/978-88-470-2463-2

Barnamehei, H., Ghomsheh, F. T., Cherati, A. S., Pouladian, M., Aminishahsavarani, A., & Golfeshan, N. (2022). Comparison between methods to create the leg length discrepancy (LLD) patient-specific model: Musculoskeletal modeling. *Biosystems and Biorobotics*, *28*(Lld), 65–69. https://doi.org/10.1007/978-3-030-70316-5_11

Bedo, B. L. S., Catelli, D. S., Lamontagne, M., & Santiago, P. R. P. (2020). A custom musculoskeletal model for estimation of medial and lateral tibiofemoral contact forces during tasks with high knee and hip flexions. *Computer Methods in Biomechanics and Biomedical Engineering*, *23*(10), 658–663. https://doi.org/10.1080/10255842.2020.1757662

Benjamini, Y., & Hochberg, Y. (1995). Controlling the false discovery rate: A practical and powerful approach to multiple testing. *Journal of the Royal Statistical Society: Series B (Methodological)*, *57*(1), 289–300. https://doi.org/10.1111/j.2517-6161.1995.tb02031.x

Bennett, H. J., Fleenor, K., & Weinhandl, J. T. (2018). A normative database of hip and knee joint biomechanics during dynamic tasks using anatomical regression prediction methods. *Journal of Biomechanics*, *81*, 122–131. https://doi.org/10.1016/j.jbiomech.2018.10.003

Bennett, H. J., Shen, G., Weinhandl, J. T., & Zhang, S. (2016). Validation of the greater trochanter method with radiographic measurements of frontal plane hip joint centers and knee mechanical axis angles and two other hip joint center methods. *Journal of*

Biomechanics, *49*(13), 3047–3051. https://doi.org/10.1016/j.jbiomech.2016.06.013

Bennett, H. J., Trypuc, A., Valenzuela, K. A., & Sievert, Z. A. (2020). Wearing knee sleeves during back squats does not improve mass lifted or affect knee biomechanics. *Human Movement*. http://repositorio.unan.edu.ni/2986/1/5624.pdf

Besomi, M., Hodges, P. W., Clancy, E. A., Van Dieën, J., Hug, F., Lowery, M., Merletti, R., Søgaard, K., Wrigley, T., Besier, T., Carson, R. G., Disselhorst-Klug, C., Enoka, R. M., Falla, D., Farina, D., Gandevia, S., Holobar, A., Kiernan, M. C., McGill, K., … Tucker, K. (2020). Consensus for experimental design in electromyography (CEDE) project: Amplitude normalization matrix. *Journal of Electromyography and Kinesiology*, *53*(June), 102438. https://doi.org/10.1016/j.jelekin.2020.102438

Bini, R., Lock, M., & Hommelhoff, G. (2021). Lower limb muscle and joint forces during front and back squats performed on a Smith machine. *Isokinetics and Exercise Science*, *29*(2), 163–173. https://doi.org/10.3233/IES-202168

Bolgla, L. A., & Uhl, T. L. (2007). Reliability of electromyographic normalization methods for evaluating the hip musculature. *Journal of Electromyography and Kinesiology*, *17*(1), 102–111. https://doi.org/10.1016/j.jelekin.2005.11.007

Boozari, S., Sanjari, M. A., Amiri, A., & Ebrahimi Takamjani, I. (2020). Fatigue effects on the viscoelastic behavior of men and women in a landing task: a Mass–Spring–Damper modeling approach. *Computer Methods in Biomechanics and Biomedical Engineering*, *23*(10), 564–570. https://doi.org/10.1080/10255842.2020.1749271

Bordron, O., Huneau, C., Le Carpentier, É., & Aoustin, Y. (2021). Human squat motion: joint torques estimation with a 3d model and a sagittal model. *Mechanisms and Machine Science*, *93*, 247–255. https://doi.org/10.1007/978-3-030-58104-6_28

Braidot, A. A., Brusa, M. H., Lestussi, F. E., & Parera, G. P. (2007). Biomechanics of front and back squat exercises. *Journal of Physics: Conference Series*, *90*(1), 1–8. https://doi.org/10.1088/1742-6596/90/1/012009

Brandon, R., Howatson, G., Strachan, F., & Hunter, A. M. (n.d.). Neuromuscular response differences to power versus strength back squat exercise in elite athletes. *Unpublished*.

Bryanton, M. A., Carey, J. P., Kennedy, M. D., & Chiu, L. Z. F. (2015). Quadriceps effort during squat exercise depends on hip extensor muscle strategy. *Sports Biomechanics*, *14*(1), 122–138. https://doi.org/10.1080/14763141.2015.1024716

Bryanton, M., Kennedy, M., Carey, J., & Chiu, L. (2012). Effect of squat depth and barbell load on relative muscular effort in squatting. *Journal of Strength and Conditioning Research*, 2820–2828. http://journals.lww.com/nsca-jscr/Abstract/publishahead/Effect_of_Squat_Depth_and_Barbell_Load_on_Relative.98097.aspx

Burden, A. (2010). How should we normalize electromyograms obtained from healthy participants? What we have learned from over 25 years of research. *Journal of Electromyography and Kinesiology*, *20*(6), 1023–1035. https://doi.org/10.1016/j.jelekin.2010.07.004

Burden, A., & Bartlett, R. (1999). Normalisation of EMG amplitude: An evaluation and comparison of old and new methods. *Medical Engineering and Physics*, *21*(4), 247–257. https://doi.org/10.1016/S1350-4533(99)00054-5

Burden, A. M., Trew, M., & Baltzopoulos, V. (2003). Normalisation of gait EMGs: A re-examination. *Journal of Electromyography and Kinesiology*, *13*(6), 519–532. https://doi.org/10.1016/S1050-6411(03)00082-8

Butler, A. B., Caruntu, D. I., & Freeman, R. A. (2017). Knee joint biomechanics for various ambulatory exercises using inverse dynamics in Opensim. *ASME International Mechanical Engineering Congress and Exposition, Proceedings (IMECE)*, *3*, 1–8. https://doi.org/10.1115/IMECE2017-70988

Catelli, D., Luiz, B., Bedo, S., Roberto, P., Santiago, P., & Lamontagne, M. (2019). Comparing forward to inverse frameworks to obtain hip joint kinematics during a squat task. *Gait & Posture*, *73*(December), 297–298. https://doi.org/10.1016/j.gaitpost.2019.07.328

Catelli, D. S. (2018). *Femoroacetabular impingement syndrome and total hip arthroplasty : Joint biomechanics before and after surgery*. http://hdl.handle.net/10393/38638

Catelli, D. S., Ng, K. C. G., Wesseling, M., Kowalski, E., Jonkers, I., Beaulé, P. E., & Lamontagne, M. (2020). Hip muscle forces and contact loading during squatting after cam-type FAI surgery. *The Journal of Bone and Joint Surgery. American Volume*, *102*, 34–42. https://doi.org/10.2106/JBJS.20.00078

Catelli, D. S., Wesseling, M., Jonkers, I., & Lamontagne, M. (2019). A musculoskeletal model customized for squatting task. *Computer Methods in Biomechanics and Biomedical Engineering*, *22*(1), 21–24. https://doi.org/10.1080/10255842.2018.1523396

Caterisano, A., Raymond, F., Pellinger, T. K., Lewis, V. C., Booth, W., Science, E., & Highway, P. (2002). The effect of back squat depth on the EMG activity of 4 superficial hip and thigh muscles. *Journal of Strength and Conditioning Research*, *16*(3), 428–432.

Chapman, A. R., Vicenzino, B., Blanch, P., Knox, J. J., & Hodges, P. W. (2010). Intramuscular fine-wire electromyography during cycling: Repeatability, normalisation and a comparison to surface electromyography. *Journal of Electromyography and Kinesiology*, *20*(1), 108–117. https://doi.org/10.1016/j.jelekin.2008.11.013

Chuang, T. D., & Acker, S. M. (2019). Comparing functional dynamic normalization methods to maximal voluntary isometric contractions for lower limb EMG from walking, cycling and running. *Journal of Electromyography and Kinesiology*, *44*(July 2018), 86–93. https://doi.org/10.1016/j.jelekin.2018.11.014

Clark, D. R., Lambert, M. I., & Hunter, A. M. (2012). Muscle activation in the loaded free barbell squat: A brief review. *The Journal of Strength and Conditioning Research*, *26*(4), 1169–1178.

Clarys, J. P. (2000). Electromyography in sports and occupational settings: An update of its limits and possibilities. *Ergonomics*, *43*(10), 1750–1762. https://doi.org/10.1080/001401300750004159

Cohen, J. (1988). *Statistical power analysis for the behavioral sciences* (Lawrence Erlbaum (ed.); 2nd editio).

Contreras, B., Vigotsky, A. D., Schoenfeld, B. J., Beardsley, C., & Cronin, J. (2015). A comparison of gluteus maximus, biceps femoris, and vastus lateralis EMG amplitude in the parallel, full, and front squat variations in resistance trained females. *Journal of Applied Biomechanics*, *31*(6), 452–458. https://doi.org/10.1123/jab.2015-0113

Coyne, L. M., Newell, M., Hoozemans, M. J. M., Morrison, A., & Brown, S. J. (2021). Marker location and knee joint constraint affect the reporting of overhead squat kinematics in elite youth football players. *Sports Biomechanics*, *00*(00), 1–18. https://doi.org/10.1080/14763141.2021.1890197

Dahlkvist, N. J., Mayo, P., & Seedhom, B. B. (1982). Forces during squatting and rising from a deep squat. *Engineering in Medicine*, *11*(2), 69–76. https://doi.org/10.1243/EMED_JOUR_1982_011_019_02

Davis III, R. B., Õunpuu, S., Tyburski, D., & Gage, J. R. (1991). A gait analysis data collection and reduction technique. *Human Movement Science*, *10*, 575–597.

De Luca, C. J. (1997). The use of surface electromyography in biomechanics. *Journal of Applied Biomechanics*, *13*, 333–342.

De Luca, C. J., Donald Gilmore, L., Kuznetsov, M., & Roy, S. H. (2010). Filtering the surface EMG signal: Movement artifact and baseline noise contamination. *Journal of Biomechanics*, *43*(8), 1573–1579. https://doi.org/10.1016/j.jbiomech.2010.01.027

Deaux, E., & Engstrom, R. (1973). The temperature of ingested water: Its effect on body temperature. *Physiological Psychology*, *1*(2), 152–154. https://doi.org/10.3758/BF03326891

Delp, S. L., Anderson, F. C., Arnold, A. S., Loan, P., Habib, A., John, C. T., Guendelman, E., & Thelen, D. G. (2007). OpenSim: Open-source software to create and analyze dynamic simulations of movement. *IEEE Transactions on Biomedical Engineering*, *54*(11), 1940–1950. https://doi.org/10.1109/TBME.2007.901024

Delp, S. L., & Zajac, F. E. (1992). Force- and moment-generating capacity of lower-extremity muscles before and after tendon lengthening. *Clinical Orthopaedics*, *284*, 247–259.

Demers, E., Pendenza, J., Radevich, V., & Preuss, R. (2018). The effect of stance width and anthropometrics on joint range of motion in the lower extremities during a back squat. *International Journal of Exercise Science*, *11*(1), 764–775. http://www.ncbi.nlm.nih.gov/pubmed/29997725%0Ahttp://www.pubmedcentral.nih.gov/articlerender.fcgi?artid=PMC6033510

Diggin, D., O'Regan, C., Whelan, N., Daly, S., Mcloughlin, V., Mcnamara, L., & Reilly, A. (2011). A biomechanical analysis of front and back squat: injury implications. *Portuguese Journal of Sports Sciences*, *11*(2001), 643–646.

Dorn, T. W., Schache, A. G., & Pandy, M. G. (2012). Muscular strategy shift in human running: Dependence of running speed on hip and ankle muscle performance. *Journal of Experimental Biology*, *215*(11), 1944–1956. https://doi.org/10.1242/jeb.064527

Duncan, M. J., Weldon, A., & Price, M. J. (2014). The effect of sodium bicarbonate ingestion on back squat and bench press exercise to failure. *Journal of Strength and Conditioning Research*, *28*(5), 1358–1366. https://doi.org/10.1519/JSC.0000000000000277

Earp, J. E., Karaemer, W. J., Newton, R. U., Comstock, B. A., Fragala, M. S., Dunn-Lewis, C., Solomon-Hill, G., Penwell, Z. R., Powell, M. D., Volek, K. S., Denegar, C. R., Häkkinen, K., & Maresh, C. M. (2010). Lower-body muscle structure and its role in jump performance during squat, countermovement, and depth drop jumps. *Journal of Strength and Conditioning Research*, *24*(3), 722–729.

Eberhart, H., Inman, V., & Bresler, B. (1954). The principal elements in human locomotion. In P. Klopsteg & P. Wilson (Eds.), *Human limbs and their substitutes* (pp. 437–471). McGraw-Hill.

Elliott, B. C., Wilson, G. J., & Kerr, G. K. (1989). A biomechanical analysis of the sticking region in the bench press. *Medicine and Science in Sports and Exercise*, *21*(4), 450–462.

Endo, Y., Miura, M., & Sakamoto, M. (2020). The relationship between the deep squat movement and the hip, knee and ankle range of motion and muscle strength. *Journal of Physical Therapy Science*, *32*(6), 391–394. https://doi.org/10.1589/jpts.32.391

Escamilla, R. F., Fleisig, G. S., Lowry, T. M., Barrentine, S. W., & Andrews, J. R. (2001). A three-dimensional biomechanical analysis of the squat during varying stance widths. *Medicine and Science in Sports and Exercise*, *33*(6), 984–998.

Escamilla, R. F., Fleisig, G. S., Zheng, N., Lander, J. E., Barrentine, S. W., Andrews, J. R.,

Bergemann, B. W., & Moorman III, C. T. (2001). Effects of technique variations on knee biomechanics during the squat and leg press. *Medicine and Science in Sports and Exercise*, *33*(9), 1552–1566. https://doi.org/10.1097/00005768-200109000-00020

Escamilla, R. F., Francisco, A. C., Fleisig, G. S., Barrentine, S. W., Welch, C. M., Kayes, A. V, Speer, K. P., & Andrews, J. R. (2000). A three-dimensional biomechanical analysis of sumo and conventional style deadlifts. *Medicine and Science in Sports and Exercise*, *32*(7), 1265–1275.

Eslava, J., Ibañez, J., Ratamess, N. A., Häkkinen, K., Asiain, X., Izquierdo, M., Altadill, A., French, D. N., Gorostiaga, E. M., Kraemer, W. J., & González-Badillo, J. J. (2006). Differential effects of strength training leading to failure versus not to failure on hormonal responses, strength, and muscle power gains. *Journal of Applied Physiology*, *100*(5), 1647–1656. https://doi.org/10.1152/japplphysiol.01400.2005

Fernandes de Oliveira, L., & Luporini Menegaldo, L. (2010). Individual-specific muscle maximum force estimation using ultrasound for ankle joint torque prediction using an EMG-driven Hill-type model. *Journal of Biomechanics*, *43*(14), 2816–2821. https://doi.org/10.1016/j.jbiomech.2010.05.035

Fiorentino, N. M., Rehorn, M. R., Chumanov, E. S., Thelen, D. G., & Blemker, S. S. (2014). Computational models predict larger muscle tissue strains at faster sprinting speeds. *Medicine and Science in Sports and Exercise*, *46*(4), 776–786. https://doi.org/10.1038/jid.2014.371

Flanagan, S. P., Kulik, J. B., & Salem, G. J. (2015). The limiting joint during a failed squat: A biomechanics case series. *Journal of Strength and Conditioning Research*, *29*(11), 3134–3142.

Flanagan, S. P., & Salem, G. J. (2008). Lower extremity joint kinetic responses to external resistance variations. *Journal of Applied Biomechanics*, *24*(1), 58–68. https://doi.org/10.1123/jab.24.1.58

Flanagan, S. P., Salem, G. J., Wang, M. Y., Sanker, S. E., & Greendale, G. A. (2003). Squatting exercises in older adults: Kinematic and kinetic comparisons. *Medicine and Science in Sports and Exercise*, *35*(4), 635–643. https://doi.org/10.1249/01.MSS.0000058364.47973.06

Fry, A. C., Smith, J. C., & Schilling, B. K. (2003). Effect of knee position on hip and knee torques during the barbell squat. *Journal of Strength and Conditioning Research*, *17*(4), 629–633. https://doi.org/10.1519/1533-4287(2003)017<0629:EOKPOH>2.0.CO;2

Fuglsang, E. I., Telling, A. S., & Sørensen, H. (2017). Effect of ankle mobility and segment ratios on trunk lean in the barbell back squat. *The Journal of Strength and Conditioning Research*, *31*(11), 3024–3033.

Gene-Morales, J., Flandez, J., Juesas, A., Gargallo, P., Miñana, I., & Colado, J. C. (2020). A systematic review on the muscular activation on the lower limbs with five different variations of the squat exercise. *Journal of Human Sport and Exercise*, *15*(Proc4), 1277–1299. https://doi.org/10.14198/jhse.2020.15.Proc4.28

Gerus, P., Rao, G., & Berton, E. (2015). Ultrasound-based subject-specific parameters improve fascicle behaviour estimation in Hill-type muscle model. *Computer Methods in Biomechanics and Biomedical Engineering*, *18*(2), 116–123. https://doi.org/10.1080/10255842.2013.780047

Golfeshan, N., Barnamehei, H., Torabigoudarzi, M., Karimidastjerdi, M., Panahi, A., Darman, A., Razaghi, M., Kharazi, M. R., Barnamehei, M., & Azad Jafarloo, S. (2020). Upper body

postures effect on neuromuscular activities of the lower limb during a squat:

musculoskeletal modeling. *Gait & Posture*, *81*(September), 107–108.

https://doi.org/10.1016/j.gaitpost.2020.07.087

Golfeshan, N., Barnamehei, M., Rezaei, A., Barnamehei, H., Kharazi, M. R., & M.A. Safaei.

(2020). Muscles kinetics effect on the generation of proximal to distal tasks: simulation of

the knife hand block movement via OpenSim. *Gait & Posture*, *81*(September), 109–110.

https://doi.org/10.1016/j.gaitpost.2020.07.088

Gomes, J., Neto, T., Vaz, J. R., Schoenfeld, B. J., & Freitas, S. R. (2020). Is there a relationship

between back squat depth, ankle flexibility, and Achilles tendon stiffness? *Sports

Biomechanics*, *00*(00), 1–14. https://doi.org/10.1080/14763141.2019.1690569

Goodman, W. W. (2020). *Thesis - Support moment distribution and induced acceleration

analysis of the barbell back squat* (Issue April).

Gorsuch, J., Long, J., Miller, K., Primeu, K., Rutledge, S., Sossong, A., & Durocher, J. J. (2013).

The effect of squat depth on multiarticular muscle activation in collegiate cross-country

runners. *The Journal of Strength and Conditioning Research*, *27*(9), 2619–2625.

Gullett, J. C., Tillman, M. D., Gutierrez, G. M., & Chow, J. W. (2009). A biomechanical

comparison of back and front squats in healthy trained individuals. *Journal of Strength and

Conditioning Research*, *23*(1), 284–292.

Haff, G. G., & Triplett, N. T. (2016). Essentials of strength training and conditioning, 4th

edition. In *National Strength and Conditioning Association: Vol. Fourth Edi*.

https://doi.org/10.1249/mss.0000000000001081

Hales, M. E., Johnson, B. F., & Johnson, J. T. (2009). Kinematic analysis of the powerlifting

style squat and the conventional deadlift during competition: is there a cross-over effect

between lifts? *Journal of Strength and Conditioning Research*, *23*(9), 2574–2580.

Hammond, B., Marques-Bruna, P., Chauhan, E., & Bridge, C. (2016). Electromyographic activity in superficial muscles of the thigh and hip during the back squat to three different depths with relative loading. *Journal of Fitness Research*, *5*(3), 57–67.

Hamner, S. R., Seth, A., & Delp, S. L. (2010). Muscle contributions to propulsion and support during running. *Journal of Biomechanics*, *43*(14), 2709–2716. https://doi.org/10.1016/j.jbiomech.2010.06.025

Hemmerich, A., Brown, H., Smith, S., & Marthandam, S. S. K. (2006). Hip, knee and ankle kinematics of high range of motion activities of daily living. *Journal of Orthopaedic Research*, *April*, 770–781. https://doi.org/10.1002/jor

Heredia, C., Lockie, R. G., Lynn, S. K., & Pamukoff, D. N. (2021). Comparison of lower extremity kinematics during the overhead deep squat by functional movement screen score. *Journal of Sports Science and Medicine*, *20*(4), 759–765. https://doi.org/10.52082/jssm.2021.759

Herrmann, A. M., & Delp, S. L. (1999). Moment arm and force-generating capacity of the extensor carpi ulnaris after transfer to the extensor carpi radialis brevis. *Journal of Hand Surgery*, *24*(5), 1083–1090. https://doi.org/10.1053/jhsu.1999.1083

Hershler, C., & Milner, M. (1978). An optimality criterion for processing electromyographic (EMG) signals relating to human locomotion. *IEEE Transactions on Biomedical Engineering*, *BME-25*(5), 413–420. https://doi.org/10.1109/TBME.1978.326338

Hicks, J. L., Uchida, T. K., Seth, A., Rajagopal, A., & Delp, S. L. (2015). Is my model good enough? Best practices for verification and validation of musculoskeletal models and simulations of movement. *Journal of Biomechanical Engineering*, *137*(2), 1–24.

https://doi.org/10.1115/1.4029304

Hirata, R., & Duarte, M. (2007). Effect of relative knee position on internal mechanical loading
while squatting. *Brazilian Journal of Physical Therapy*, *11*(2), 107–111.
http://www.scielo.br/scielo.php?pid=S1413-35552007000200006&script=sci_arttext

Horsak, B., Pobatschnig, B., Schwab, C., Baca, A., Kranzl, A., & Kainz, H. (2018). Reliability of
joint kinematic calculations based on direct kinematic and inverse kinematic models in
obese children. *Gait and Posture*, *66*(August), 201–207.
https://doi.org/10.1016/j.gaitpost.2018.08.027

Jaberzadeh, S., Yeo, D., & Zoghi, M. (2016). The effect of altering knee position and squat depth
on VMO : VL EMG ratio during squat exercises. *Physiotherapy Research International*,
21(3), 164–173. https://doi.org/10.1002/pri.1631

Jung, Y., Koo, Y., & Koo, S. (2017). *Simultaneous estimation of ground reaction force and knee
contact force during walking and squatting*. *18*(9), 1263–1268.
https://doi.org/10.1007/s12541-017-0148-7

Karabulut, D., Dogru, S. C., Lin, Y. C., Pandy, M. G., Herzog, W., & Arslan, Y. Z. (2020).
Direct validation of model-predicted muscle forces in the cat hindlimb during locomotion.
Journal of Biomechanical Engineering, *142*(5). https://doi.org/10.1115/1.4045660

Kashiwagi, K., Tanaka, M., Kawazoe, T., Furuichi, K., & Takada, H. (1995). Effect of amplitude
normalization on surface EMG linear envelopes of masticatory muscles during gum
chewing. *Journal of Osaka Dental University*, *29*(1), 19–28.
https://doi.org/10.18905/jodu.29.1_19

Kipp, K., & Kim, H. (2021). Force-length-velocity behavior and muscle-specific joint moment
contributions during countermovement and squat jumps. *Computer Methods in*

Biomechanics and Biomedical Engineering, *0*(0), 1–10.

https://doi.org/10.1080/10255842.2021.1973446

Kipp, K., Kim, H., & Wolf, W. I. (2022a). Muscle-specific contributions to lower extremity net

joint moments while squatting with different external loads. *Journal of Strength and

Conditioning Research*, *36*(2), 324–331. https://doi.org/10.1519/JSC.0000000000003874

Kipp, K., Kim, H., & Wolf, W. I. (2022b). Muscle forces during the squat, split squat, and step-

up across a range of external loads in college-aged men. *Journal of Strength and

Conditioning Research*, *36*(2), 314–323. https://doi.org/10.1519/jsc.0000000000003688

Knutson, L. M., Soderberg, G. L., Ballantyne, B. T., & Clarke, W. R. (1994). A study of various

normalization procedures for within day electromyographic data. *Journal of

Electromyography and Kinesiology*, *4*(1), 47–59. https://doi.org/10.1016/1050-

6411(94)90026-4

Kompf, J., & Arandjelović, O. (2016). Understanding and overcoming the sticking point in

resistance exercise. *Sports Medicine*, *46*(6), 751–762. https://doi.org/10.1007/s40279-015-

0460-2

Kompf, J., & Arandjelović, O. (2017). The sticking point in the bench press, the squat, and the

deadlift: Similarities and differences, and their significance for research and practice. *Sports

Medicine*, *47*(4), 631–640. https://doi.org/10.1007/s40279-016-0615-9

Konrad, P. (2006). *ABC of EMG a practical introduction to kinesiological electromyography*

(1st Editio, Issue March). Noraxon, Inc.

Korak, A., Bruininks, B., & Paquette, M. (2020). The influence of normalization technique on

between-muscle activation during a back-squat. *Medicine & Science in Sports & Exercise*,

52(7S), 673–673. https://doi.org/10.1249/01.mss.0000682500.56692.37

Kramer, P. A., Feuerriegel, E. M., Lautzenheiser, S. G., & Sylvester, A. D. (2022). Sensitivity of

    musculoskeletal models to variation in muscle architecture parameters. *Evolutionary*

    Human Sciences, 1–31. https://doi.org/10.1017/ehs.2022.6

Kubo, T., Hirayama, K., Nakamura, N., & Higuchi, M. (2018). Influence of different loads on

    force-time characteristics during back squats. *Journal of Sports Science and Medicine*,

    17(4), 617–622.

Lai, A. K. M., Arnold, A. S., Wakeling, J. M., Biology, E., & Station, C. F. (2017). Why are

    antagoist muscle co-activated in my simulation? A musculoskeletal model for analysing

    human locomotor tasks. *Annals of Biomedical Engineering*, *45*(12), 2762–2774.

    https://doi.org/10.1007/s10439-017-1920-7.Why

Lamas, M., Mouzo, F., Michaud, F., Lugris, U., & Cuadrado, J. (2022). Comparison of several

    muscle modeling alternatives for computationally intensive algorithms in human motion

    dynamics. *Multibody System Dynamics*, 415–442. https://doi.org/10.1007/s11044-022-

    09819-y

Li, X., Adrien, N., Baker, J. S., Mei, Q., & Gu, Y. (2021). Novice female exercisers exhibited

    different biomechanical loading profiles during full-squat and half-squat practice. *Biology*,

    10(11), 1–12.

Lin, Y. C., Walter, J. P., Banks, S. A., Pandy, M. G., & Fregly, B. J. (2010). Simultaneous

    prediction of muscle and contact forces in the knee during gait. *Journal of Biomechanics*,

    43(5), 945–952. https://doi.org/10.1016/j.jbiomech.2009.10.048

Lorenzetti, S., Gülay, T., Stoop, M., List, R., Gerber, H., Schellenbert, F., & Stüssi, E. (2012).

    Comparison of the angles and corresponding moments in the knee and hip during restricted

    and unrestricted squats. *Journal of Strength and Conditioning Research*, *26*(10), 2892–

2836.

Lu, Y., Mei, Q., Peng, H. Te, Li, J., Wei, C., & Gu, Y. (2020). A comparative study on loadings of the lower extremity during deep squat in Asian and Caucasian individuals via OpenSim musculoskeletal modelling. *BioMed Research International*, *2020*. https://doi.org/10.1155/2020/7531719

Lu, Z., Li, X., Rong, M., Baker, J. S., & Gu, Y. (2022). Effect of rearfoot valgus on biomechanics during barbell squatting: A study based on OpenSim musculoskeletal modeling. *Frontiers in Neurorobotics*, *16*. https://doi.org/10.3389/fnbot.2022.832005

Lynn, S. K., & Noffal, G. J. (2012). Lower extremity biomechanics during a regular and counterbalanced squat. *Journal of Strength and Conditioning Research*, *26*(9), 2417–2425.

Mackala, K., Stodólka, J., Siemienski, A., & Ćoh, M. (2013). Biomechanical analysis of squat jump and countermovement jump from varying starting positions. *Journal of Strength and Conditioning Research*, *27*(10), 2650–2661.

Maddox, E. U., & Bennett, H. J. (2021). Effects of external load on sagittal and frontal plane lower extremity biomechanics during back squats. *Journal of Biomechanical Engineering*, *143*(5), 1–10. https://doi.org/10.1115/1.4049747

Maddox, E. U., Bennett, H. J., & Weinhandl, J. T. (2022). Evidence for the use of dynamic maximum normalization method of muscle activation during weighted back squats. *Journal of Biomechanics*, *135*(March), 111029. https://doi.org/10.1016/j.jbiomech.2022.111029

Maddox, E. U., Sievert, Z. A., & Bennett, H. J. (2020). Modified vector coding analysis of trunk and lower extremity kinematics during maximum and sub-maximum back squats. *Journal of Biomechanics*, *106*, 109830. https://doi.org/10.1016/j.jbiomech.2020.109830

Mantovani, G., & Lamontagne, M. (2017). How Different Marker Sets Affect Joint Angles in

Inverse Kinematics Framework. *Journal of Biomechanical Engineering*, *139*(4), 1–7. https://doi.org/10.1115/1.4034708

Marchetti, P. H., da Silva, J. J., Schoenfeld, B. J., Nardi, P. S. M., Pecoraro, S. L., Greve, J. M. D., & Hartigan, E. (2016). Muscle activation differs between three different knee joint-angle positions during a maximal isometric back squat exercise. *Journal of Sports Medicine*, 1–6. https://doi.org/10.1155/2016/3846123

Marshall, P. W. M., McEwen, M., & Robbins, D. W. (2011). Strength and neuromuscular adaptation following one, four, and eight sets of high intensity resistance exercise in trained males. *European Journal of Applied Physiology*, *111*(12), 3007–3016. https://doi.org/10.1007/s00421-011-1944-x

McBride, J. M., Blow, D., Kirby, T. J., Haines, T. L., Dayne, A. M., & Triplett, N. T. (2009). Relationship between maximal squat strength and five, ten, and forty yard sprint times. *The Journal of Strength and Conditioning Research*, *23*(6), 1633–1636.

McConnell, J., Donnelly, C., Hamner, S., Dunne, J., & Besier, T. (2011). Effect of shoulder taping on maximum shoulder external and internal rotation range in uninjured and previously injured overhead athletes during a seated throw. *Journal of Orthopaedic Research*, *29*(9), 1406–1411. https://doi.org/10.1002/jor.21399

McCurdy, K., O'Kelley, E., Kutz, M., Langford, G., Ernest, J., & Torres, M. (2010). Comparison of lower extremity EMG between the 2-leg squat and modified single-leg squat in female athletes. *Journal of Sport Rehabilitation*, *19*(1), 57–70. https://doi.org/10.1123/jsr.19.1.57

Mehls, K., Grubbs, B., Jin, Y., & Coons, J. (2020). Electromyography comparison of sex differences during the back squat. *Journal of Strength and Conditioning Research*, 1. https://doi.org/10.1519/jsc.0000000000003469

Merletti, R., & Muceli, S. (2019). Tutorial. Surface EMG detection in space and time: Best practices. *Journal of Electromyography and Kinesiology*, *49*(October), 102363. https://doi.org/10.1016/j.jelekin.2019.102363

Miletello, W. M., Beam, J. R., & Cooper, Z. C. (2009). A biomechanical analysis of the squat between competitive collegiate, competitive high school, and novice powerlifters. *Journal of Strength and Conditioning Research*, *23*(5), 1611–1617.

Modenese, L., & Renault, J. B. (2021). Automatic generation of personalised skeletal models of the lower limb from three-dimensional bone geometries. *Journal of Biomechanics*, *116*, 110186. https://doi.org/10.1016/j.jbiomech.2020.110186

Mokhtarzadeh, H., Perraton, L., Fok, L., Muñoz, M. A., Clark, R., Pivonka, P., & Bryant, A. L. (2014). A comparison of optimisation methods and knee joint degrees of freedom on muscle force predictions during single-leg hop landings. *Journal of Biomechanics*, *47*(12), 2863–2868. https://doi.org/10.1016/j.jbiomech.2014.07.027

Murray, N., Cipriani, D., O'Rand, D., & Reed-Jones, R. (2013). Effects of foot position during squatting on the quadriceps femoris: an electromyographic study. *International Journal of Exercise Science*, *6*(2), 114–125. http://search.ebscohost.com/login.aspx?direct=true&profile=ehost&scope=site&authtype=crawler&jrnl=1939795X&AN=87560766&h=Taqpm2x8i5jyJRVd7twdj8q4aHXZkEOUYX7E6A89q7Kvq+g17ttNWTeiXM+GoIExMnYisbq70vhhDv8WaFie5w==&crl=c

Myer, G. D., Jushner, A. M., Brent, J. L., Schoenfeld, B. J., Hugentobler, J., Lloyd, R. S., Vermeil, A., Chu, D. A., Harbin, J., & McGill, S. M. (2014). The back squat: a proposed assessment of functional defecits and technical factors that limit performance. *Strength and Conditioning Journal*, *1*(36), 4–27. https://doi.org/10.1519/SSC.0000000000000103.The

Nakagawa, T. H., Moriya, É. T. U., Maciel, C. D., & Serrão, F. V. (2012). Trunk, pelvis, hip, and knee kinematics, hip strength, and gluteal muscle activation during a single-leg squat in males and females with and without patellofemoral pain syndrome. *Journal of Orthopaedic & Sports Physical Therapy*, *42*(6), 491–501. https://doi.org/10.2519/jospt.2012.3987

Niu, W., Wang, Y., He, Y., Fan, Y., & Zhao, Q. (2010). Biomechanical gender differences of the ankle joint during simulated half-squat parachute landing. *Aviation Space and Environmental Medicine*, *81*(8), 761–767. https://doi.org/10.3357/ASEM.2725.2010

Orjalo, A., Moreno, M., Birmingham-Babauta, S., Stage, A., Callaghan, S., Stokes, J., Giuliano, D., Davis, D., Lazar, A., Risso, F., Lockie, R., & Liu, T. (2017). An investigation of the mechanics and sticking region of a one-repetition maximum close-grip bench press versus the traditional bench press. *Sports*, *5*(4), 46. https://doi.org/10.3390/sports5030046

Panariello, R. A., Backus, S. I., & Parker, J. W. (1994). The effect of the squat exercise on anterior-posterior knee translation in professional football players. *The American Journal of Sports Medicine*, *22*(6), 768–773. https://doi.org/10.1177/036354659402200607

Pangan, A. M., & Leineweber, M. (2021). Footwear and elevated heel influence on barbell back squat: A review. *Journal of Biomechanical Engineering*, *143*(9), 1–10. https://doi.org/10.1115/1.4050820

Park, S., Caldwell, G. E., & Umberger, B. R. (2022). A direct collocation framework for optimal control simulation of pedaling using OpenSim. *PLoS ONE*, *17*(2 February), 1–17. https://doi.org/10.1371/journal.pone.0264346

Pataky, T. C., Caravaggi, P., Savage, R., Parker, D., Goulermas, J. Y., Sellers, W. I., & Crompton, R. H. (2008). New insights into the plantar pressure correlates of walking speed using pedobarographic statistical parametric mapping (pSPM). *Journal of Biomechanics*,

41(9), 1987–1994. https://doi.org/10.1016/j.jbiomech.2008.03.034

Portney, L. G., & Watkins, M. P. (2000). *Foundations of clinical research: Applications to practice* (3rd Editio). Prentice Hall Health.

Rajagopal, A., Dembia, C. L., DeMers, M. S., Delp, D. D., Hicks, J. L., & Delp, S. L. (2016). Full body musculoskeletal model for muscle-driven simulation of human gait. *IEEE Transactions on Biomedical Engineering*, *62*(10), 2068–2079. https://doi.org/10.1109/TBME.2016.2586891.Full

Reinbolt, J. A., Seth, A., & Delp, S. L. (2011). Simulation of human movement: Applications using OpenSim. *Procedia IUTAM*, *2*, 186–198. https://doi.org/10.1016/j.piutam.2011.04.019

Ricard, M. D., Ugrinowitsch, C., Parcell, A. C., Hilton, S., Rubley, M. D., Sawyer, R., & Poole, C. R. (2005). Effects of rate of force development on EMG amplitude and frequency. *International Journal of Sports Medicine*, *26*(1), 66–70. https://doi.org/10.1055/s-2004-817856

Riemer, R., & Hsiao-Wecksler, E. T. (2008). Improving joint torque calculations: Optimization-based inverse dynamics to reduce the effect of motion errors. *Journal of Biomechanics*, *41*(7), 1503–1509. https://doi.org/10.1016/j.jbiomech.2008.02.011

Roberts, B. M., Nuckols, G., & Krieger, J. W. (2020). Sex differences in resistance training: A systematic review and meta-analysis. *Journal of Strength and Conditioning Research*, *34*(5), 1448–1460. https://doi.org/10.1519/JSC.0000000000003521

Sanborn, K., Boros, R., Hruby, J., Schilling, B., O'Bryant, H. S., Johnson, R. L., Hoke, T., Stone, M. E., & Stone, M. H. (2000). Short-term performance effects of weight training with multiple sets not to failure vs. a single set to failure in women. *Journal of Strength and*

Conditioning Research, *14*(3), 328–331.

Schache, A. G., Wrigley, T. V., Baker, R., & Pandy, M. G. (2009). Biomechanical response to hamstring muscle strain injury. *Gait and Posture*, *29*(2), 332–338. https://doi.org/10.1016/j.gaitpost.2008.10.054

Schellenberg, F., Taylor, W. R., Trepczynski, A., List, R., Kutzner, I., Schütz, P., Duda, G. N., & Lorenzetti, S. (2018). Evaluation of the accuracy of musculoskeletal simulation during squats by means of instrumented knee prostheses. *Medical Engineering and Physics*, *61*, 95–99. https://doi.org/10.1016/j.medengphy.2018.09.004

Schoenfeld, B. J. (2010). Squatting kinematics and kinetics and their application to exercise performance. *Journal of Strength and Conditioning Research*, *24*(12), 3497–3506. https://doi.org/10.1519/JSC.0b013e3181bac2d7

Seitz, L. B., Reyes, A., Tran, T. T., de Villarreal, E. S., & Haff, G. G. (2014). Increases in lower-body strength transfer positively to sprint performance: A systematic review with meta-analysis. *Sports Medicine*, *44*(12), 1693–1702. https://doi.org/10.1007/s40279-014-0227-1

Seth, A., Reinbolt, J. A., & Delp, S. L. (2004). *Musculoskeletal modeling: How it began, what it offers, and where it is heading*. 2–4.

Seth, A., Sherman, M., Reinbolt, J. A., & Delp, S. L. (2011). OpenSim: A musculoskeletal modeling and simulation framewrk for in silico investigations and echange. *Procedia IUTAM*, *2*, 212–232. https://doi.org/10.1016/j.piutam.2011.04.021.OpenSim

Shelburne, K. B., & Pandy, M. G. (2002). A dynamic model of the knee and lower limb for simulating rising movements. *Computer Methods in Biomechanics and Biomedical Engineering*, *5*(2), 149–159. https://doi.org/10.1080/10255840290010265

Sinclair, J., Taylor, P. J., Shadwell, G., Stone, M., Booth, N., Jones, B., Finlay, S., Ali, A. M.,

Butters, B., Bentley, I., & Edmundson, C. J. (2022). Two-experiment examination of habitual and manipulated foot placement angles on the kinetics, kinematics, and muscle forces of the barbell back squat in male lifters. *Sensors*, *22*(18), 1–21. https://doi.org/10.3390/s22186999

Singh, D., & Padgham, L. (2014). OpenSim: A framework for integrating agent-based models and simulation components. *Frontiers in Artificial Intelligence and Applications*, *263*, 837–842. https://doi.org/10.3233/978-1-61499-419-0-837

Smale, K. B., Conconi, M., Sancisi, N., Krogsgaard, M., Alkjaer, T., Parenti-Castelli, V., & Benoit, D. L. (2019). Effect of implementing magnetic resonance imaging for patient-specific OpenSim models on lower-body kinematics and knee ligament lengths. *Journal of Biomechanics*, *83*, 9–15. https://doi.org/10.1016/j.jbiomech.2018.11.016

Song, K., Pascual-Garrido, C., Clohisy, J. C., & Harris, M. D. (2022). Elevated loading at the posterior acetabular edge of dysplastic hips during double-legged squat. *Journal of Orthopaedic Research*, *November 2021*, 1–9. https://doi.org/10.1002/jor.25249

Spoor, C. W., & Veldpaus, F. E. (1980). Rigid body motion calculated from spatial co-ordinates of markers. *Journal of Biomechanics*, *13*(4), 391–393.

Stearns, K. M., Keim, R. G., & Powers, C. M. (2013). Influence of relative hip and knee extensor muscle strength on landing biomechanics. *Medicine and Science in Sports and Exercise*, *45*(5), 935–941. https://doi.org/10.1249/MSS.0b013e31827c0b94

Suydam, S. M., Manal, K., & Buchanan, T. S. (2017). The advantages of normalizing electromyography to ballistic rather than isometric or isokinetic tasks. *Journal of Applied Biomechanics*, *33*(3), 189–196. https://doi.org/10.1123/jab.2016-0146

van den Tillaar, R. (2015). Kinematics and muscle activation around the sticking region in free-

weight barbell back squats. *Kinesiologia Slovenica*, *21*(1), 15–25.

van den Tillaar, R., Andersen, V., & Saeterbakken, A. H. (2014). The existence of a sticking region in free weight squats. *Journal of Human Kinetics*, *42*(1), 63–71. https://doi.org/10.2478/hukin-2014-0061

Vigotsky, A. D., Halperin, I., Lehman, G. J., Trajano, G. S., & Vieira, T. M. (2018). Interpreting signal amplitudes in surface electromyography studies in sport and rehabilitation sciences. *Frontiers in Physiology*, *8*(JAN). https://doi.org/10.3389/fphys.2017.00985

Wan, X., Qu, F., Garrett, W. E., Liu, H., & Yu, B. (2017). Relationships among hamstring muscle optimal length and hamstring flexibility and strength. *Journal of Sport and Health Science*, *6*(3), 275–282. https://doi.org/10.1016/j.jshs.2016.04.009

Waters, R. L., Perry, J., McDaniels, J. M., & House, K. (1974). The relative strength of the hamstrings during hip extension. *Journal of Bone and Joint Surgery - Series A*, *56*(8), 1592–1597. https://doi.org/10.2106/00004623-197456080-00006

Weinhandl, J. T., Irmischer, B. S., & Bennett, H. J. (2021). The effects of sex and landing task on hip mechanics. *Computer Methods in Biomechanics and Biomedical Engineering*. https://doi.org/10.1080/10255842.2021.1921163

Weinhandl, J. T., Joshi, M., & O'Connor, K. M. (2010). Gender comparisons between unilateral and bilateral landings. *Journal of Applied Biomechanics*, *26*(4), 444–453. https://doi.org/10.1123/jab.26.4.444

Willardson, J. M. (2007). The application of training to failure in periodized multiple-set resistance exercise programs. *Journal of Strength and Conditioning Research*, *21*(2), 628–631. https://doi.org/10.1519/R-20426.1

Williams, M. J., Gibson, N. V., Sorbie, G. G., Ugbolue, U. C., Brouner, J., & Easton, C. (2021).

Activation of the Gluteus Maximus During Performance of the Back Squat, Split Squat, and Barbell Hip Thrust and the Relationship With Maximal Sprinting. In *Journal of strength and conditioning research* (Vol. 35, Issue 1). https://doi.org/10.1519/JSC.0000000000002651

Wolf, W. I., Kim, H., & Kipp, K. (2021). Musculoskeletal modelling based estimates of load dependent relative muscular effort during resistance training exercises. *Sports Biomechanics*. https://doi.org/10.1080/14763141.2021.1983636

Xie, K., Lyu, Y., Zhang, X., & Song, R. (2021). How compliance of surfaces affects ankle moment and stiffness regulation during walking. *Frontiers in Bioengineering and Biotechnology*, *9*(October), 1–10. https://doi.org/10.3389/fbioe.2021.726051

Yang, J. F., & Winter, D. A. (1984). Electromyographic amplitude normalization methods: Improving their sensitivity as diagnostic tools in gait analysis. *Archives of Physical Medicine and Rehabilitation*, *65*(9), 517–521.

Yavuz, H. U., Erdağ, D., Amca, A. M., & Aritan, S. (2015). Kinematic and EMG activities during front and back squat variations in maximum loads. *Journal of Sports Sciences*, *33*(10), 1058–1066. https://doi.org/10.1080/02640414.2014.984240

Youdas, J. W., Hollman, J. H., Hitchcock, J. R., Hoyme, G. J., & Johnsen, J. J. (2007). Comparison of hamstring and quadriceps femoris electromyographic activity between men and women during a single-limb squat on both a stable and labile surface. *Journal of Strength and Conditioning Research*, *12*(1), 105–111.

Zawadka, M., Smolka, J., Skublewska-Paszkowska, M., Lukasik, E., & Gawda, P. (2020). How are squat timing and kinematics in the sagittal plane related to squat depth? *Journal of Sports Science and Medicine*, *19*(3), 500–507.

Zeller, B. L., Mccrory, J. L., Kibler, W. Ben, & Uhl, T. L. (2003). Differences in kinematics and

electromyographic activity between men and women during the single-legged squat. *The

American Journal of Sports Medicine*, *31*(3), 449–456.

VITA

EVA MARIA URDIALES MADDOX

Education

Doctor of Philosophy
        Old Dominion University, Virginia
        Conferred: December 2022
        Human Movement Sciences
        Concentration: Applied Kinesiology
        Specialization: Biomechanics
        Dissertation Topic: A biomechanical analysis of back squats: motion capture,
                        electromyography, and musculoskeletal modeling

Master of Science
        San Francisco State University, California
        Conferred: May 2015
        Cellular and Molecular Biology
        Thesis Topic: Development of an in vitro assay for the Membrane Bound O-Acyl
                        Transferase, Porcupine.

Bachelor of Science
        Austin Peay State University, Tennessee
        Conferred: May 2013
        Biology

Publications

Maddox, E.U., Bennett, H.J., Weinhandl, J.T. (2022). Evidence for the use of dynamic maximum normalization method of muscle activation during weighted back squats. *Journal of Biomechanics*.

Galli, L.M., Anderson, M.O., Fraley, J.G., Sanchez, L., Bueno, R., **Maddox, E.U.,** Lingappa, V., Burrus, L.W. (2021) Determination of the membrane topology of PORCN, an O-acyl transferase that modifies Wnt signaling proteins. *Royal Society Open Biology.*

Maddox, E.U., Bennett, H.J. (2021). Effects of external load on sagittal and frontal plane lower extremity biomechanics during back squats. *Journal of Biomechanical Engineering*.

Maddox, E.U., Sievert, Z.A., Bennett, H.J. (2020). Modified vector coding analysis of trunk and lower extremity kinematics during maximum and sub-maximum back squats. *Journal of Biomechanics*, 106.

Gienger, C.M., **Urdiales, E.M.** (2017). Influences on standard metabolism in Eastern Box Turtles *(Terrapene carolina). Chelonian Conservation and Biology*, 16(2), 159-163.